Infectious Disease Modelling 9 (2024) 103–127

Contents lists available at ScienceDirect

Infectious Disease Modelling

journal homepage: www.keaipublishing.com/idm

Dynamics of a two-group model for assessing the impacts of pre-exposure prophylaxis, testing and risk behaviour change on the spread and control of HIV/AIDS in an MSM population

Queen Tollett [a], Salman Safdar [b], Abba B. Gumel [c, d, *]

[a] School of Mathematical and Statistical Sciences, Arizona State University, Tempe, AZ, 85287, USA
[b] Department of Mathematics, University of Karachi, University Road, 75270, Pakistan
[c] Department of Mathematics, University of Maryland, College Park, MD, 20742, USA
[d] Department of Mathematics and Applied Mathematics, University of Pretoria, Pretoria, 0002, South Africa

ARTICLE INFO

Article history:
Received 13 September 2023
Received in revised form 9 November 2023
Accepted 10 November 2023
Available online 20 November 2023
Handling Editor: Dr Daihai He

Keywords:
HIV/AIDS
MSM
High(low)-risk groups
PrEP
Behavior change
Antiviral treatment
Control reproduction number

ABSTRACT

Although much progress has been made in reducing the public health burden of the human immunodeficiency virus (HIV), which causes acquired immunodeficiency syndrome (AIDS), since its emergence in the 1980s (largely due to the large-scale use and availability of potent antiviral therapy, improved diagnostic and intervention and mitigation measures), HIV remains an important public health challenge globally, including in the United States. This study is based on the use of mathematical modeling approaches to assess the population-level impact of pre-exposure prophylaxis (PrEP), voluntary testing (to detect undetected HIV-infected individuals), and changes in human behavior (with respect to risk structure), on the spread and control of HIV/AIDS in an MSM (men-who-have sex-with-men) population. Specifically, a novel two-group mathematical model, which stratifies the total MSM population based on risk (low or high) of acquisition of HIV infection, is formulated. The model undergoes a PrEP-induced backward bifurcation when the *control reproduction number* of the model is less than one if the efficacy of PrEP to prevent a high-risk susceptible MSM individual from acquiring HIV infection is not perfect (the consequence of which is that, while necessary, having the reproduction number of the model less than one is no longer sufficient for the elimination of the disease in the MSM population). For the case where the efficacy of PrEP is perfect, this study shows that the disease-free equilibrium of the two-group model is globally-asymptotically stable when the associated control reproduction number of the model is less than one. Global sensitivity analysis was carried out to identify the main parameters of the model that have the highest influence on the value of the control reproduction number of the model (thereby, having the highest influence on the disease burden in the MSM population). Numerical simulations of the model, using a plausible range of parameter values, show that if half of the MSM population considered adhere strictly to the specified PrEP regimen (while other interventions are maintained at their baseline values), a reduction of about 22% of the new yearly HIV cases recorded at the peak of the disease could be averted (compared to the *worst-case scenario* where PrEP-based intervention is not implemented in the MSM population). The yearly reduction at the peak increases to about 50% if the PrEP coverage in the MSM population increases to 80%. This study showed, based on the parameter values used in the simulations, that the prospects of elimination of HIV/AIDS in the MSM community

* Corresponding author. Department of Mathematics, University of Maryland, College Park, MD, 20742, USA.
E-mail address: agumel@umd.edu (A.B. Gumel).
Peer review under responsibility of KeAi Communications Co., Ltd.

https://doi.org/10.1016/j.idm.2023.11.004

are promising if high-risk susceptible individuals are no more than 15% more likely to acquire HIV infection, in comparison to their low-risk counterparts. Furthermore, these prospects are significantly improved if undetected HIV-infected individuals are detected within an optimal period of time.

1. Introduction

The human immunodeficiency virus (HIV), the causative agent of acquired immunodeficiency syndrome (AIDS), remains a significant global public health and socio-economic concern since its emergence in the early 1980s (the disease accounts for 1.5 million new infections and 1 million deaths globally each year (Our World in Data, 2019)). Approximately 39 million people currently live with HIV/AIDS (Kaiser Family Foundation, 2020; U.S. Department of Health & Human Services, 2023; UNAIDS, 2023), and 40% of new HIV infections are transmitted by people who are unaware of their HIV infection status (Centers for Disease Control and Prevention, 2020a). AIDS is associated with a gradual decline and failure of the immune system of the infected individual, leading to significant weight loss, often accompanied by diarrhea, chronic weakness, fever, and eventually increases the risk of numerous (opportunistic) life-threatening infections (Mayo Clinic, 2022).

Although the primary mode of HIV transmission is sexual (through contact with infected bodily fluids), the disease can also be transmitted vertically (during pregnancy or childbirth, or through breastfeeding) (Centers for Disease Control and Prevention, 2020b) and *via* non-sexual routes, such as needle sharing by *intravenous drug users* (IDUs), and blood transfusion (Centers for Disease Control and Prevention, 2020b). To cause transmission, infected bodily fluids must come in contact with mucous membranes or damaged tissue or be injected directly into the bloodstream of the susceptible person (Simpson & Gumel, 2017). HIV in the United States is predominantly prevalent in the sub-populations of *men-who-have-sex-with-men* (MSM), IDUs, or MSM who are also IDUs and in heterosexual sex worker communities (Centers for Disease Control and Prevention, 2020c; Simpson & Gumel, 2017). In the United States (and worldwide), MSM of all races and ethnicities currently have the highest incidence of HIV, and remain the group most severely (and disproportionately) affected by the disease (Centers for Disease Control and Prevention, 2021a). Furthermore, "the estimated lifetime risk for HIV/AIDS infection among the MSM population in the United States is one in six, compared with heterosexual men at one in 524 and heterosexual women at one in 253" (Centers for Disease Control and Prevention, 2021a; National Institutes of Health, 2021).

Numerous preventive and therapeutic strategies are being implemented in an effort to effectively control and mitigate the spread of HIV/AIDS in the United States (Centers for Disease Control and Prevention, 2020b). Some of the main preventive strategies include the use of condoms during sexual intercourse, mass testing to detect HIV-infected individuals (including asymptomatically infected individuals), HIV screening for pregnant women (as part of a routine antenatal screening to avoid vertical transmission), public health education and counselling against risky practices that could result in the acquisition or transmission of HIV infection (as well as the acquisition or transmission of other sexually transmitted infections), access to sterile needles and injecting equipment (Centers for Disease Control and Prevention, 2020b; NHS, 2021) and the use of *pre-exposure prophylaxis* (PrEP) (Centers for Disease Control and Prevention, 2020b; NHS, 2021) (post-exposure prophylaxis (PEP), taken within 72 hours after a recent possible exposure to HIV, is also being used). The main therapeutic treatment strategy is the use of *antiretroviral treatment* (ART). Although the aforementioned control strategies have helped curb the spread of the disease, it remains a significant public health and socioeconomic challenge in the United States (Simpson & Gumel, 2017) (the Centers for Disease Control and Prevention (CDC) estimates that the lifetime treatment cost for an individual infected with HIV in the United States is $379,668 (in 2010) (Bingham et al., 2021; Centers for Disease Control and Prevention, 2022a)). PrEP is considered to be a promising preventive strategy to end the AIDS epidemic, and is the subject of focus for the current study.

The United States Food and Drug Administration (FDA) approved two drugs, namely *Truvada* and *Descovy*, for PrEP (with Truvada approved in 2012, while Descovy was approved in 2016 (U.S. Department of Health & Human Services, 2022; Food and Drug Administration, 2019)). Each of these drugs (taken by people who are HIV negative) is in pill form and must be taken once a day in conjunction with condom use during sexual contact to be more effective (U.S. Department of Health & Human Services, 2022). Individuals on these drugs are regularly tested for HIV (every three months). Furthermore, both drugs have *emtricitabine*, but *Truvada* combines it with *tenefovir disoproxifumarate* while *Descovy* combines it with *tenofovir alafenamide* (Biktarvy. Biktarvy, 2022). While *Truvada* is generally recommended for individuals who are at risk for HIV through sex and *IDU*, *Descovy* is only recommended for individuals who are at risk of HIV infection through sex (U.S. Department of Health & Human Services, 2022; U.S. Department of Health & Human Services, 2021a). CDC data show that consistent use of PrEP medication could lead to a 99% reduction in the risk of acquiring HIV infection by sex and reduce the risk of HIV from intravenous drug use by at least 74%, compared to those who did not take them consistently (Centers for Disease Control and Prevention, 2023) (see also (Centers for Disease Control and Prevention, 2022b; STDcenterNY. Everything you need to, 2022)). Unfortunately, despite the overall progress in curbing the HIV/AIDS pandemic through the use of pharmaceutical interventions, the disease continues to affect some groups severely and disproportionately in the United States. This is largely due to persistent inequity in PrEP usage. For instance, in the year 2021 alone, only 9% (42,372) of the nearly 469,000 Black

people who could benefit from PrEP received a prescription, and only 16% (48,838) of the nearly 313,000 Hispanic/Latino people (who could benefit from PrEP) received a prescription (Centers for Disease Control and Prevention, 2021b). Inequities also exists in PrEP prescription and usage by gender. During 2020, for example, PrEP coverage was about three times higher among men (28%), compared to women (10%) (Centers for Disease Control and Prevention, 2021b). These inequities in the prescription and use of PrEP (by ethnicity and gender) translate into an increased incidence of HIV in ethnic minority and female populations (Centers for Disease Control and Prevention, 2021b).

Several mathematical models, typically in the form of deterministic systems of nonlinear differential equations, have been developed and used to assess the impact of PrEP on the transmission dynamics and control of HIV/AIDS in both homosexual (Mitchell et al., 2014; Simpson & Gumel, 2017) and heterosexual (Nsuami & Peter, 2018; Omondi et al., 2018; Sun et al., 2014; Supervie et al., 2011) populations. For instance, Simpson et al. (Simpson & Gumel, 2017) presented a stage-progression model for HIV/AIDS to assess the population-level impact of the use of PrEP on the transmission dynamics of the disease in an MSM population. This study reported that the effective disease control can be achieved in the MSM community of Minnesota if $[61 - 77\%]$ of susceptible members of the MSM community are on PrEP (Simpson & Gumel, 2017). Mitchell et al. (Mitchell et al., 2014) modeled the population-level impact of PrEP for FSWs and MSM on HIV incidence and survival in Southern India. This study showed that PrEP (even with 60% efficacy and 40% coverage in the targeted populations) could prevent over 20% of new infections in the targeted populations. Supervie et al. (Supervie et al., 2011) investigated the potential impact of PrEP intervention on reducing HIV infections within the MSM community in San Francisco, as well as its potential to significantly increase transmitted resistance. Kim et al. (Sun et al., 2014) reported that PrEP and early diagnosis could be a very effective way to curb HIV incidence among the MSM community in South Korea (Sun et al., 2014). Nsuami et al. (Nsuami & Peter, 2018) showed that while managing HIV with early treatment can decrease transmission, increase in the uptake of PrEP could significantly reduce the number of overall HIV/AIDS infections in South Africa. Finally, Omondi et al. (Omondi et al., 2022) showed that increase in PrEP uptake could lead to a decline in the number of HIV/AIDS patients on antiretroviral therapy.

The current study introduces a two-group model for the transmission dynamics of HIV/AIDS in an MSM community in the State of Arizona. The model to be developed, which incorporates the main epidemiological and biological features of the disease (such as the stage-progression property of the transmission process), will be used to assess the population-level impact of the three pillars of the United States Anti-HIV Initiative to reduce HIV infections in the country by 90% by 2030 (Centers for Disease Control and Prevention, 2021c; U.S. Department of Health & Human Services, 2021b) (namely HIV testing, antiretroviral therapy and PrEP) in combating and mitigating the spread of the disease in an MSM population in the State of Arizona. Another novel feature of the model to be designed is that it stratifies the total MSM population according to risk of acquisition of HIV infection. That is, we split the total MSM population into those who are low- or high-risk of acquiring an HIV infection (based on how much risk they take in their sexual practices). The paper is organized as follows. The two-group, risk-structured model is formulated in Section 2. The model is fitted using yearly case data for HIV in an MSM population in the State of Arizona in this section. Rigorous analysis of the model, with respect to the existence and asymptotic stability properties of its disease-free and endemic equilibria, is explored in Section 3. The feasibility of the dynamic phenomenon of *backward bifurcation* is also rigorously explored in this section. Global uncertainty and parameter sensitivity analyses are carried out in section 4. Numerical simulations, as well as global parameter sensitivity analyses, are reported in Section 5. The results of this study are summarized in Section 6.

2. Model formulation

The model to be developed in this study is that of HIV/AIDS transmission dynamics and control in an MSM community in the State of Arizona. In the formulation of the model, the main mode of transmission to be considered is sexual (*albeit* intravenous drug use is also an important mode of transmission in this group). Furthermore, the total susceptible MSM population will be stratified according to the risk of acquisition of HIV infection. Specifically, the susceptible population will be divided into two risk groups, low and high. The susceptible high-risk population consists of HIV negative MSM individuals who, in addition to having sexual contacts with HIV-positive individuals, are *intravenous drug users*. The low-risk, susceptible group consists of HIV-negative MSM who do not engage in risky sexual (or IDU) behavior. In addition to the risk structure, another notable feature of HIV disease to be incorporated into the model is the stage structure (namely, the primary stage, the secondary stage, and the AIDS stage). Furthermore, in addition to PrEP and treatment (given to the sexually active susceptible MSM individuals), another important feature to be included into the model is voluntary testing. The motivation for this is that a sizable percentage of HIV-infected individuals in the U.S. are unaware of their infection status. To account for this (i.e., testing and detection), the infected MSM population will be stratified based on whether they know their infection status. In other words, we will classify the MSM infected individuals in terms of whether they are detected (*via* testing) or not. In this study, three main preventive and therapeutic strategies against HIV/AIDS are considered, namely the use of PrEP to prevent susceptible MSM individuals from acquiring an HIV infection, voluntary testing aimed at detecting infected individuals who are unaware of their infection status and the treatment (using antiretroviral therapy) for those who have been detected (i.e., those who are aware of their infection status). In the model to be developed, PrEP is only administered to susceptible individuals in the high-risk category. Based on the above descriptions, the total MSM population at time t, denoted by $N(t)$, is sub-divided into the mutually-exclusive compartments of low-risk susceptible ($S_L(t)$), and high-risk susceptible ($S_H(t)$), individuals in the primary stage of infection who are unaware ($I_{1_u}(t)$) or aware ($I_{1_d}(t)$) of their infection status, individuals in

the secondary stage who are unaware ($I_{2u}(t)$) or aware ($I_{2d}(t)$) of their infection status, individuals in the AIDS stage of infection who are unaware ($A_u(t)$) or aware ($A_d(t)$) of their infection status and effectively treated infected individuals ($T(t)$). Thus,

$$N(t) = S_L(t) + S_H(t) + I_{1u}(t) + I_{1d}(t) + I_{2u}(t) + I_{2d}(t) + A_u(t) + A_d(t) + T(t).$$

The risk-structured and staged-structured model for HIV transmission in an MSM population (where PrEP, antiretroviral drugs and testing are administered and implemented as preventive and/or therapeutic interventions) is given by the following deterministic system of nonlinear differential equations. The flow diagram of the model (2.1) is shown in Fig. 1, and the description of the state variables and parameters of the model is tabulated in Tables 1 and 2, respectively:

$$\begin{cases}
\frac{dS_L}{dt} = \Pi(1-p) + \psi_H S_H - \lambda(t) S_L - \psi_L S_L - \mu S_L, \\
\frac{dS_H}{dt} = \Pi p + \psi_L S_L - \eta_H(1-\epsilon_p c_p)\lambda(t) S_H - \psi_H S_H - \mu S_H, \\
\frac{dI_{1u}}{dt} = \lambda(t) S_L + \eta_H(1-\epsilon_p c_p)\lambda(t) S_H - \epsilon_d \xi_d I_{1u} - \sigma_{1u} I_{1u} - \mu I_{1u}, \\
\frac{dI_{1d}}{dt} = \epsilon_d \xi_d I_{1u} - \tau_1 I_{1d} - \sigma_{1d} I_{1d} - \mu I_{1d}, \\
\frac{dI_{2u}}{dt} = \sigma_{1u} I_{1u} - \epsilon_d \xi_d I_{2u} - \sigma_{2u} I_{2u} - \mu I_{2u}, \\
\frac{dI_{2d}}{dt} = \epsilon_d \xi_d I_{2u} + \sigma_{1d} I_{1d} - \tau_2 I_{2d} - \sigma_{2d} I_{2d} - \mu I_{2d}, \\
\frac{dA_u}{dt} = \sigma_{2u} I_{2u} - \epsilon_d \xi_d A_u - \mu A_u - \delta_u A_u, \\
\frac{dA_d}{dt} = \sigma_{2d} I_{2d} + \epsilon_d \xi_d A_u - \tau_A A_d - \mu A_d - \delta_d A_d, \\
\frac{dT}{dt} = \tau_I I_{1d} + \tau_2 I_{2d} + \tau_A A_d - \mu T,
\end{cases} \tag{2.1}$$

where the *force of infection*, $\lambda(t)$, is given by

$$\lambda(t) = \beta \frac{[I_{1u}(t) + \eta_d I_{1d}(t) + \eta_2\{I_{2u}(t) + \eta_d I_{2d}(t)\} + \eta_A\{A_u(t) + \eta_d A_d(t)\}]}{N(t)}. \tag{2.2}$$

In the model (2.1), Π is the rate at which new sexually-active MSM individuals are recruited into the population (assumed to be susceptible), and a proportion, $0 \leq p < 1$, of these are assumed to be high-risk susceptible individuals. Low (high)-risk susceptible individuals change their risk behavior and become high (low)-risk at a rate of $\psi_H(\psi_L)$. Susceptible individuals acquire HIV infection at the rate $\lambda(t)$, given by model (2.1). In Equation (2.2), β is the effective contact rate, $0 < \eta_d < 1$ is the modification parameter for the assumed reduced infectiousness of detected individuals, in relation to undetected individuals

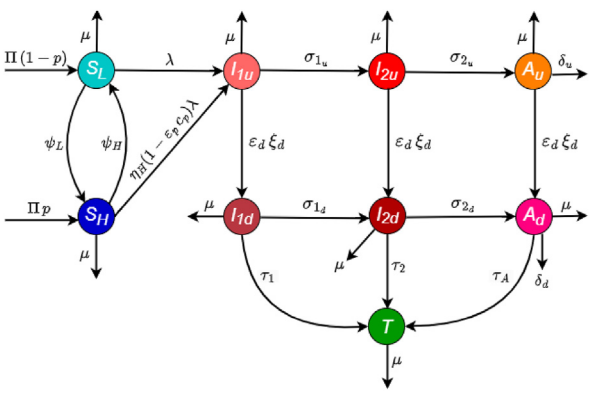

Fig. 1. Flow diagram of the two-group model (2.1), for the dynamics of HIV/AIDS in an MSM population (Tollett, 2023).

Table 1
Description of the state variables of the two-group model (2.1) for the dynamics of HIV/AIDS in an MSM population(Tollett, 2023).

State Variable	Description
S_L	Population of low-risk susceptible individuals
S_H	Population of high-risk susceptible individuals
I_{1u}	Population of undetected HIV-infected individuals in primary stage of infection
I_{1d}	Population of detected HIV-infected individuals in primary stage of infection
I_{2u}	Population of undetected HIV-infected individuals in secondary stage of infection
I_{2d}	Population of detected HIV-infected individuals in secondary stage of infection
A_u	Population of undetected HIV-infected individuals in AIDS stage of infection
A_d	Population of detected HIV-infected individuals in AIDS stage of infection
T	Population of successfully-treated individuals

(since they are on treatment, therefore they have reduced viral load), $0 < \eta_2 < 1$ is the modification parameter for the reduced infectiousness of individuals in the secondary stage of infection, in relation to those in the primary stage of infection (owing to their reduced viral load), and $\eta_A > 0$ is the modification parameter accounting for the variability of infectiousness of individuals in the AIDS stage of infection, in relation to those in the primary stage of infection (η_A could be less than or greater than unity). Natural mortality occurs in each epidemiological compartment at a rate μ. High-risk susceptible individuals acquire HIV infection at a rate $\eta_H(1 - \varepsilon_p c_p)\lambda$, where $\eta_H > 1$ is the modification parameter for the assumed increase in the likelihood of acquiring an HIV infection by high-risk susceptible individuals, in relation to low-risk susceptible individuals (due to their high-risk sexual practices), $0 < \varepsilon_p < 1$ is the efficacy of PrEP in preventing infection and $0 < c_p \leq 1$ is compliance in PrEP usage. Infected individuals who are unaware of their infection status (i.e., those in $I_{1u}(t)$, $I_{2u}(t)$ and $A_u(t)$ classes) are detected, after voluntary testing, at a rate $\varepsilon_d\, \xi_d$, where ξ_d is the testing/detection rate and $1 < \varepsilon_d \leq 2$ is the efficacy of the diagnostic test (PCR) administered. Individuals in the primary stage progress to the corresponding secondary stage ($I_{2u}(t)$) at a rate σ_{1u}. Detected individuals in the primary infection stage (i.e., those in the $I_{1d}(t)$ class) are treated at a rate τ_1 and progress to the corresponding secondary stage ($I_{2d}(t)$) at a rate σ_{1d}. Undetected infected individuals in the secondary stage of infection ($I_{2u}(t)$) progress to the corresponding AIDS stage of infection ($A_u(t)$) at a rate σ_{2u}. Similarly, those in the ($I_{2d}(t)$) class progress to the ($A_d(t)$) class at a rate σ_{2d}. Individuals in this ($I_{2d}(t)$) class are treated at a rate τ_2. The treatment rate of detected individuals in the AIDS stage of infection is denoted by τ_A. Individuals in the ($A_u(A_d)$) stage of HIV infection die due to opportunistic infections associated with AIDS, at a rate $\delta_u(\delta_d)$ (Tollett, 2023). The main assumptions made in the formulation of the model (2.1) are:

1. Homogeneous mixing (i.e., a well-mixed MSM population, where every member of the population has equal likelihood of mixing with every other member; and that individuals are indistinguishable).
2. Exponentially distributed waiting time in each epidemiological compartment.
3. For mathematical tractability, it is assumed that the detection rate and efficacy of the diagnostic test implemented are the same in all undetected infected compartments.
4. Effectively-treated infected individuals do not transmit infection or die of the disease.

2.1. Basic qualitative properties

In this section we assess the well-posedness of the model (2.1). We define the following biologically-feasible region for the model (2.1):

$$\Gamma = \left\{ (S_L, S_H, I_{1u}, I_{1d}, I_{2u}, I_{2d}, A_u, A_d, T) \in \mathbb{R}^9_+ : 0 \leq N \leq \frac{\Pi}{\mu} \right\}.$$

We claim the following result:

Theorem 2.1. *Consider the two-group model (2.1) with non-negative initial conditions. The region Γ is positively-invariant and attracts all solutions of the model (2.1).*

Proof. *Adding all the equations of the model* (2.1) *gives* (Tollett, 2023):

$$\frac{dN}{dt} = \Pi - \mu N - \delta_u A_u - \delta_d A_d, \tag{2.3}$$

thereby (since all state variables and parameters of the model are non-negative)

Table 2
Description of parameters of the model (2.1) (Tollett, 2023).

Parameter	Description
Π	Recruitment rate into the sexually-active MSM population
$0 \leq p < 1$	Proportion of newly sexually-active susceptible individuals that are high-risk
β	Effective contact rate
$\psi_L(\psi_H)$	Transition rate from low(high)-risk to high(low)-risk susceptible population
μ	Natural death rate
$0 < \eta_d < 1$	Modification parameter for reduced infectiousness of detected individuals, in relation to undetected individuals
$0 < \eta_2 < 1$	Modification parameter for the reduced infectiousness of individuals in secondary stage of infection, in relation to those in primary stage
$\eta_A > 0$	Modification parameter for the variables of infectiousness of individuals in the AIDS stage of infection, in relation to those in primary stage
$\eta_H > 1$	Modification parameter for the assumed increase in the likelihood of acquiring an HIV infection by high-risk susceptible individuals
$0 < \varepsilon_p < 1$	Efficacy of PrEP to prevent acquisition of HIV infection
$0 < c_p \leq 1$	Compliance in PrEP usage
$\sigma_{1u}(\sigma_{1d})$	Progression rate of undetected (detected) individuals in primary stage to the corresponding secondary stage
$\sigma_{2u}(\sigma_{2d})$	Progression rate of undetected (detected) individuals in secondary stage to the corresponding AIDS stage
ξ_d	Detection rate of diagnostic test administered
$1 < \varepsilon_d \leq 2$	Efficacy of diagnostic test to detect undetected individuals
$\tau_1(\tau_2)$	Treatment rate of detected individuals in $I_{1d}(I_{2d})$ class
τ_A	Treatment rate of detected individuals in AIDS stage of infection
$\delta_u(\delta_d)$	Disease-induced mortality rate of undetected (detected) individuals in the AIDS stage

$$\frac{dN}{dt} \leq \Pi - \mu N. \tag{2.4}$$

Hence if $N \leq \frac{\Pi}{\mu}$, then $\frac{dN}{dt} \leq 0$. Thus, it follows, by applying a standard comparison theorem (Lakshmikantham & Leela, 1969), that:

$$N(t) \leq \frac{\Pi}{\mu} + \left[N(0) - \frac{\Pi}{\mu}\right] e^{-\mu t}. \tag{2.5}$$

In particular, $N(t) \leq \frac{\Pi}{\mu}$ if $N(0) \leq \frac{\Pi}{\mu}$. Further, if $N(t) > \frac{\Pi}{\mu}$, then $dN(t)/dt < 0$. Therefore, every solution of the model (2.1) with initial conditions in Γ remains in Γ for all time. Thus, the region Γ is positively-invariant and attracting (Tollett, 2023; J Brozak et al., 2021). □

Since the region Γ is positively-invariant, attracting and bounded, it is therefore sufficient to study the dynamics of the model (2.1) therein (Hethcote, 2000) (in this region, the model is mathematically and epidemiologically well-posed).

2.2. Data fitting and parameter estimation

The two-group model (2.1) contains several parameters (i.e., 23 parameters). The values of 19 parameters are known from the available literature (as tabulated in Table 5), while the values of the remaining four parameters (namely; β, ψ_l, ψ_h and τ_A) are unknown. The values of the unknown parameters are estimated by fitting the model with data. Specifically, the model (2.1) is fitted using the yearly new HIV case data for the MSM population from the State of Arizona (reported by the Arizona Department of Health Services) for the period 1990–2019 (Arizona Department of Health Services, 2015; Tollett, 2023). To fit the model with the data, we use the standard least squares approach (using the MATLAB's inbuilt minimization function, *lsqcurvefit*, to minimize the sum of the squared differences between each of the observed yearly new HIV case data points and the corresponding yearly new case points obtained from the model (2.1) (Tollett, 2023)) and a bootstrapping technique (which entails using the MATLAB's "*bootstrp*" routine to generate 10,000 bootstrap replicates needed for generating the bootsrap distribution to be used to estimate the unknown parameters (Ngonghala et al., 2021; Ngonghala et al., 2023)). The estimated values of the unknown parameters, together with the 95% credible intervals for the estimated parameters (obtained using the *prctile* routine in MATLAB) are tabulated in Table 4. The results obtained, for fitting the observed data with the model, is shown in Fig. 2 (a), showing a very good fit. The data fitting is further validated by using the estimated and fixed parameters of the model to compute the cumulative yearly new HIV cases in the MSM community, and compared with the observed cumulative case data. The results obtained, depicted in Fig. 2 (b), shows a very good fit (confirming the goodness of the fitting in Fig. 2 (a)).

3. Existence and asymptotic stability of equilibria

In this section, the model (2.1) will be rigorously analyzed to explore the conditions for the existence and asymptotic stability of disease-free equilibrium and endemic equilibrium.

Table 3
Baseline values of the parameters of the model (2.1).

Parameter	Baseline Value	Source
Π	1379	(Arizona Department of Health Services, 2021; Grey et al., 2016)
p	0.15	Pitasi et al. (2018)
σ_{1u}	0.5	Poorolajal et al. (2016)
σ_{1d}	0.5	Poorolajal et al. (2016)
σ_{2u}	0.2223	Chen et al. (2015)
σ_{2d}	0.2223	Chen et al. (2015)
ξ_d	0.8	Assumed
ε_d	1.5	Assumed
η_d	0.43	Podder et al. (2011)
η_2	0.5	Assumed
η_A	1.5	Simpson and Gumel (2017)
δ_u	0.0047	Poorolajal et al. (2016)
δ_d	0.09	Poorolajal et al. (2016)
τ_1	0.54	McCann et al. (2020)
τ_2	0.54	McCann et al. (2020)
η_H	1.5	Assumed
ε_p	0.964	Eisinger et al. (2019)
c_p	0.31	Hood et al. (2016)
μ	0.0125	Centers for Disease Control and Prevention (2022c)

3.1. Disease-free equilibrium

The model (2.1) has a disease-free equilibrium (DFE), given by:

$$\begin{aligned}\mathcal{E}_{DF} &= (S_L^*, S_H^*, 0, 0, 0, 0, 0, 0, 0)\\ &= \left(\frac{\Pi(\psi_H + (1-p)\mu}{\mu K}, \frac{\Pi(p\mu + \psi_L)}{\mu K}, 0, 0, 0, 0, 0, 0, 0\right).\end{aligned} \tag{3.1}$$

where, $K = \mu + \psi_H + \psi_L$.

The local asymptotic stability of the DFE will be explored using the next generation operator method (Diekmann & Peter Heesterbeek, 2000; van den Driessche & James, 2002). Specifically, it follows, using the notation in (van den Driessche & James, 2002), that the non-negative matrix, F, of new infection terms, and the M-matrix, V, of linear transformation terms, associated with the model (2.1), are given, respectively, by (Tollett, 2023):

$$F = \begin{bmatrix} \frac{\beta B^*}{N^*} & \eta_d\frac{\beta B^*}{N^*} & \eta_2\frac{\beta B^*}{N^*} & \eta_2\eta_d\frac{\beta B^*}{N^*} & \eta_A\frac{\beta B^*}{N^*} & \eta_A\eta_d\frac{\beta B^*}{N^*} \\ 0 & 0 & 0 & 0 & 0 & 0 \\ 0 & 0 & 0 & 0 & 0 & 0 \\ 0 & 0 & 0 & 0 & 0 & 0 \\ 0 & 0 & 0 & 0 & 0 & 0 \end{bmatrix}$$

and,

$$V = \begin{bmatrix} C_1 & 0 & 0 & 0 & 0 & 0 \\ -\epsilon_d\,\xi_d & C_2 & 0 & 0 & 0 & 0 \\ -\sigma_{1u} & 0 & C_3 & 0 & 0 & 0 \\ 0 & -\sigma_{1d} & -\epsilon_d\,\xi_d & C_4 & 0 & 0 \\ 0 & 0 & -\sigma_{2u} & 0 & C_5 & 0 \\ 0 & 0 & 0 & -\sigma_{2d} & -\epsilon_d\,\xi_d & C_6 \end{bmatrix}$$

where,

Table 4
Baseline values of the four estimated (fitted) parameters (and their confidence intervals (CIs)) of the model (2.1), obtained by fitting the model with the yearly new case data for HIV/AIDS for the State of Arizona.

Parameter	Estimated Value	95% Confidence Interval
β	0.41885 year^{-1}	[0.418856750000022 – 0.419034817481054]
ψ_l	0.43590 year^{-1}	[0.435900000000022 – 0.435900000000074]
ψ_h	0.57764 year^{-1}	[0.566971713275986 – 0.577648999999978]
τ_A	0.10145 year^{-1}	[0.101452000000022 – 0.101639654457191]

Table 5
Table of PRCC values of the parameters in the expression for the control reproduction number, $\mathbb{R}_{T_c}$, of the model (2.1). PRCC values above 0.5 in magnitude are highlighted with a (*), implying that these parameters are highly correlated (i.e., either positively-correlated or negatively-correlated with the response function). Apart from the modification parameters, (i.e., η_d, η_A, η_A and η_H), efficacies (i.e., ε_p and ε_d), the proportion "p" and the compliance parameter "c_p" which are dimensionless, all the other parameters and their ranges have unit of per year.

Parameter	Baseline Value	Range	PRCC: $\mathbb{R}_{T_c}$
β	0.4188	[0.3350, 0.5025]	0.943*
p	0.15	[0.120, 0.180]	0.3723
ψ_L	0.4359	[0.3487, 0.5230]	0.735*
ψ_H	0.5776	[0.4620, 0.6931]	−0.737*
σ_{1u}	0.5	[0.400, 0.600]	0.0653
σ_{1d}	0.5	[0.400, 0.600]	0.2053
σ_{2u}	0.222	[0.178, 0.267]	0.1594
σ_{2d}	0.222	[0.178, 0.267]	0.3719
ξ_d	0.8	[0.640, 0.960]	−0.650*
ε_d	1.5	[1.200, 1.800]	−0.661*
η_d	0.43	[0.344, 0.516]	0.845*
η_2	0.5	[0.400, 0.600]	0.4068
η_A	1.5	[1.200, 1.800]	0.601*
δ_u	0.005	[0.004, 0.006]	−0.0314
δ_d	0.09	[0.072, 0.108]	−0.3591
τ_1	0.54	[0.440, 0.640]	−0.539*
τ_2	0.54	[0.440, 0.640]	0.0166
τ_A	0.1014	[0.0811, 0.1217]	−0.3139
η_H	1.5	[1.200, 1.800]	0.916*
ε_p	0.964	[0.771, 1.157]	−0.698*
c_p	0.31	[0.248, 0.372]	−0.680*

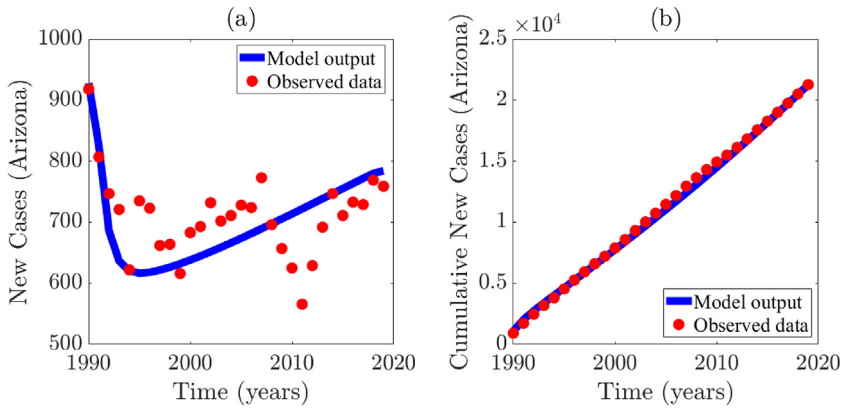

Fig. 2. (*a*) Time series illustration of the least squares fit of the model (2.1), showing the model's output for the yearly cases (blue curve) compared to the observed yearly confirmed cases for the State of Arizona (red dots) from 1990–2019. (*b*) Simulation result of the model (2.1), showing cumulative HIV/AIDS cases for the State of Arizona as a function of time (in years), using the fixed and estimated baseline parameter values as tabulated in Tables 3 and 4, respectively (Tollett, 2023).

$$B^* \quad = S_L^* + \eta_H(1-\epsilon_p c_p)S_H^*, N^* = \frac{\Pi}{\mu}, C_1 = \epsilon_d\ \xi_d + \sigma_{1u} + \mu, C_2 = \tau_1 + \sigma_{1d} + \mu, C_3 = \epsilon_d\ \xi_d + \sigma_{2u} + \mu, C_4 = \tau_2 + \sigma_{2d} + \mu,$$

$$C_5 = \epsilon_d\ \xi_d + \delta_u + \mu, \quad C_6 = \tau_A + \delta_d + \mu. \tag{3.2}$$

It is convenient to define (where ρ is the spectral radius):

$$\mathbb{R}_{T_c} = \rho(FV^{-1}) \quad = \mathbb{R}_{I_{1u}} + \mathbb{R}_{I_{1d}} + \mathbb{R}_{I_{2u}} + \mathbb{R}_{I_{2d}} + \mathbb{R}_{A_u} + \mathbb{R}_{A_d}, \tag{3.3}$$

where,

$$\mathbb{R}_{I_{1u}} \quad = \left(\frac{\beta B^*}{N^*}\right)\left(\frac{1}{C_1}\right), \quad \mathbb{R}_{I_{1d}} = \eta_d\left(\frac{\beta B^*}{N^*}\right)\left(\frac{\epsilon_d\xi_d}{C_1C_2}\right), \quad \mathbb{R}_{I_{2u}} = \eta_2\left(\frac{\beta B^*}{N^*}\right)\left(\frac{\sigma_{1u}}{C_1C_3}\right), \quad \mathbb{R}_{I_{2d}} = \eta_2\eta_d\left(\frac{\beta B^*}{N^*}\right)\left(\frac{\epsilon_d\xi_d\sigma_{1d}}{C_1C_2C_4} + \frac{\sigma_{1u}\epsilon_d\xi_d}{C_1C_3C_4}\right),$$

$$\mathbb{R}_{A_u} = \eta_A\left(\frac{\beta B^*}{N^*}\right)\left(\frac{\sigma_{1u}\sigma_{2u}}{C_1C_3C_5}\right), \quad \mathbb{R}_{A_d} = \eta_A\eta_d\left(\frac{\beta B^*}{N^*}\right)\left(\frac{\sigma_{1u}\sigma_{2u}\epsilon_d\xi_d}{C_1C_3C_5C_6} + \frac{\epsilon_d\xi_d\sigma_{1d}\sigma_{2d}}{C_1C_2C_4C_6} + \frac{\sigma_{1u}\epsilon_d\xi_d\sigma_{2d}}{C_1C_3C_4C_6}\right). \tag{3.4}$$

In (3.4), the quantities $\mathbb{R}_{I_{1u}}$,$\mathbb{R}_{I_{1d}}$,$\mathbb{R}_{I_{2u}}$,$\mathbb{R}_{I_{2d}}$,$\mathbb{R}_{A_u}$,$\mathbb{R}_{A_d}$ represent, respectively, the constituent reproduction numbers for individuals in the I_{1u}, I_{1d}, I_{2u}, I_{2d}, A_u, A_d classes. The result below follows from Theorem 2 of (van den Driessche & James, 2002).

Theorem 3.1. *The disease-free equilibrium* ($\mathcal{E}_{DF}$) *of the model (2.1) is locally-asymptotically stable whenever* $\mathbb{R}_{T_c} < 1$, *and is unstable if* $\mathbb{R}_{T_c} > 1$.The epidemiological implication of Theorem 3.1 is that a small influx of HIV-infected individuals will not generate a large outbreak in the MSM population if the quantity $\mathbb{R}_{T_c}$ can be brought to (and maintained at) a value less than one. The quantity $\mathbb{R}_{T_c}$ is the *control reproduction number* of the model (2.1). It measures the average number of new HIV cases generated by a typical infected individual introduced into the MSM population where a certain proportion of infected individuals receive anti-HIV treatment (Tollett, 2023).

3.2. Existence and asymptotic stability of endemic equilibria

In this section, we explore conditions for the existence and asymptotic stability of endemic equilibria (i.e., equilibria where the infected components of the model are nonzero) of the model (2.1).

$$\mathcal{E}_{EE} = (S_L^{**}, S_H^{**}, I_{1u}^{**}, I_{1d}^{**}, I_{2u}^{**}, I_{2d}^{**}, A_u^{**}, A_d^{**}, T^{**}) \tag{3.5}$$

represents any arbitrary (positive) endemic equilibrium point of the model (2.1) with

$$N^{**} = S_L^{**} + S_H^{**} + I_{1u}^{**} + I_{1d}^{**} + I_{2u}^{**} + I_{2d}^{**} + A_u^{**} + A_d^{**} + T^{**} \tag{3.6}$$

and the *force of infection* (λ) now defined as:

$$\lambda^{**} = \frac{\beta}{N^{**}}\{I_{1u}^{**} + \eta_d I_{1d}^{**} + \eta_2(I_{2u}^{**} + \eta_d I_{2d}^{**}) + \eta_A(A_u^{**} + \eta_d A_d^{**})\}. \tag{3.7}$$

The components of the arbitrary equilibrium (obtained by solving for each of the state variables of the model (2.1) at steady-state) are given as:

$$S_L^{**} \quad = \frac{\Pi(1-p) + \psi_H S_H^{**}}{\lambda^{**} + \psi_L + \mu}, \ S_H^{**} = \frac{\Pi p + \psi_L S_L^{**}}{\eta_H(1-\epsilon_p c_p)\lambda^{**} + \psi_H + \mu}, \ I_{1u}^{**} = \frac{\lambda^{**}\{S_L^{**} + \eta_H(1-\epsilon_p c_p)S_H^{**}\}}{C_1},$$

$$I_{1d}^{**} \quad = \frac{\epsilon_d\ \xi_d\ \lambda^{**}\{S_L^{**} + \eta_H(1-\epsilon_p c_p)S_H^{**}\}}{C_1C_2}, \ I_{2u}^{**} = \frac{\sigma_{1u}I_{1u}^{**}}{C_3}, \ I_{2d}^{**} = \frac{\epsilon_d\ \xi_d\ I_{2u}^{**} + \sigma_{1d}\ I_{1d}^{**}}{C_4}, A_u^{**} = \frac{\sigma_{2u}I_{2u}^{**}}{C_5}, \tag{3.8}$$

$$A_d^{**} = \frac{\sigma_{2d}\ I_{2d}^{**} + \epsilon_d\ \xi_d\ A_u^{**}}{C_6}, \ T^{**} = \frac{\tau_1 I_{1d}^{**} + \tau_2 I_{2d}^{**} + \tau_A A_d^{**}}{\mu}.$$

Substituting the equations in (3.8) into (3.7) yields

$$\lambda^{**} = \frac{\lambda^{**}\Pi\ \mu\ K(\ \beta\ N_1\ Q_1\lambda^{**} + \mathbb{R}_{T_c})}{[\Pi\ B_1\ D_1(\lambda^{**})^2 + \{\Pi\ \mu\ B_2\ D_2 + \Pi\ B_3\ D_1\}\lambda^{**} + \Pi\ \mu\ K\ D_2]} \tag{3.9}$$

where,

$$\begin{aligned}
N_1 &= C_2\,C_3\,C_4\,C_5\,C_6 + C_3\,C_4\,C_5\,C_6\,\eta_d\,\epsilon_d\,\xi_d + C_2\,C_4\,C_5\,C_6\,\eta_2\,\sigma_{1_u} + C_2\,C_4\,C_6\,\eta_A\,\sigma_{1_u}\,\sigma_{2_u} + C_5\,C_6\,\eta_2\,\eta_d\,\epsilon_d\,\xi_d\,\sigma_{1_u}\,(C_2 + C_3)\\
&\quad + \eta_A\,\eta_d\,\epsilon_d\,\xi_d\,(C_2C_5\,\sigma_{1_u}\sigma_{2_d} + C_3C_5\,\sigma_{1_d}\sigma_{2_d} + C_2C_4\,\sigma_{1_u}\sigma_{2_u}),\\
D_1 &= \mu\,C_2\,C_3\,C_4\,C_5\,C_6 + \mu\,C_3\,C_4\,C_5\,C_6\,\epsilon_d\,\xi_d + \mu\,C_2\,C_4\,C_5\,C_6\,\sigma_{1_u} + \mu\,C_2\,C_4\,C_6\,\sigma_{1_u}\,\sigma_{2_u}\\
&\quad + \mu\,C_5\,C_6\,\epsilon_d\,\xi_d\,(C_2\,\sigma_{1_u} + C_3\,\sigma_{1_d}) + \mu\,\epsilon_d\,\xi_d\,(C_2C_5\,\sigma_{1_u}\sigma_{2_d} + C_3C_5\,\sigma_{1_d}\sigma_{2_d} + C_2\,C_4\,\sigma_{1_u}\sigma_{2_u})\\
&\quad + C_5\,C_6\,\epsilon_d\,\xi_d\,(C_3\,C_4\,\tau_1 + C_2\,\tau_2 + C_3\,\sigma_{1_u}\,\tau_2) + \epsilon_d\,\xi_d\,\tau_A\,(C_2\,C_5\,\sigma_{1_u}\,\sigma_{2_d} + C_2\,C_4\,\sigma_{1_u}\,\sigma_{2_u} + C_3\,C_5\,\sigma_{1_d}\,\sigma_{2_d}),\\
D_2 &= C_1\,C_2\,C_3\,C_4\,C_5\,C_6, B_1 = \eta_H(1-\epsilon_p\,c_p), B_2 = \{(1-p)\eta_H(1-\epsilon_p\,c_p) + p\},\\
B_3 &= \psi_h + \mu(1-p) + \{\eta_h\,(1-\epsilon_p\,c_p)\}\,(\psi_l + \mu\,p), Q_1 = \frac{\eta_H\,(1-\epsilon_p\,c_p)}{K},\ \text{and}\ \ K = \mu + \psi_H + \psi_L.
\end{aligned} \tag{3.10}$$

It follows that the non-zero (endemic) equilibria of the model (2.1), satisfy the following polynomial (in terms of λ^{**}),

$$a_2(\lambda^{**})^2 + a_1\lambda^{**} + a_0 = 0, \tag{3.11}$$

where,

$$a_2 = \Pi\ B_1\ D_1,\ a_1 = \Pi\ \mu\ B_2\ D_2 + \Pi\ B_3\ D_1 - \Pi\ \beta\ K\ \mu\ N_1\ Q_1, a_0 = \Pi\ \mu\ K\ D_2\ (1-\mathbb{R}_{T_c}), \tag{3.12}$$

with B_1, D_1, B_2, D_2, B_3, K, N_1 as defined in (3.10). The quadratic equation (3.11) can be analyzed for the possibility of multiple endemic equilibria when $\mathbb{R}_{T_c} < 1$. It should be noted that the coefficient a_2 is always positive (since $\varepsilon_p c_p < 1$ thus $(1 - \varepsilon_p c_p) > 0$ and all the state variables are also positive) and a_0 is negative if $\mathbb{R}_{T_c} > 1$. Hence, the following result follows from the quadratic equation (3.11) (Tollett, 2023).

Theorem 3.2. *The two-group model* (2.1) *has*: (*i*) *a unique endemic equilibrium if* $a_0 < 0 \leftrightarrow \mathbb{R}_{T_c} > 1$; (*ii*) *a unique endemic equilibrium if* $a_1 < 0$, *and* $a_0 = 0$ *or* $a_1^2 - 4a_0a_2 = 0$; (*iii*) *two endemic equilibria if* $a_0 > 0$, $a_1 < 0$, *and* $a_1^2 - 4a_0a_2 > 0$; (*iv*) *no endemic equilibrium otherwise.Case* (*i*) *of* Theorem 3.2 *shows that the model* (2.1) *has a unique endemic equilibrium whenever* $\mathbb{R}_{T_c} > 1$. *Furthermore, Case* (*iii*) *of* Theorem 3.2 *suggests the possibility of backward bifurcation, a dynamic phenomenon characterized by the co-existence of multiple stable equilibria* (*a disease-free equilibrium and a stable endemic equilibrium*) *when the associated reproduction number of the model* ($\mathbb{R}_{T_c}$) *is less than unity* (Gumel, 2012). *The implication of the phenomenon of backward bifurcation is that the requirement, while necessary, is not sufficient for disease elimination. In this case, disease elimination will depend upon the initial sizes of the sub-populations of the model* (Gumel, 2012). *Accordingly, the existence of backward bifurcation in the transmission dynamics of a disease makes it difficult to achieve effective control* (*or elimination*) *of that disease in the community. The existence of such phenomenon in the model* (2.1) *will be explored now* (Tollett, 2023).

Theorem 3.3. *The model* (2.1) *undergoes a backward bifurcation at* $\mathbb{R}_{T_c} = 1$ *whenever the inequality* (*A*.11), *given in* Appendix A, *holds*.The proof of Theorem 3.3, based on using center manifold theory, is given in Appendix A. Fig. 3 depicts the backward bifurcation plots associated with the model (2.1). However, the arbitrary set of parameter values chosen to generate the backward bifurcation diagram (i.e., Fig. 3) may not be biologically meaningful but these arbitrary set of parameter values are chosen to show the phenomenon of backward bifurcation associated with the model (2.1). It should be mentioned that, for computational convenience (in generating Fig. 3), we set, the eigenvectors v_1 and v_3 in (A.3) (given in Appendix A) to one. Similarly, we set the eigenvectors w_2 and w_3 in (A.4) to one. To ensure that the effective control of the HIV/AIDS in a MSM population (or the elimination of the disease) is independent of the initial sizes of the sub-populations of the model (2.1), it is necessary that the disease-free equilibrium is proved to be globally-asymptotically stable when the associated control reproduction number of the model is less than unity. This will be explored below in Section 3.3, for the special case of the model (2.1) (Tollett, 2023).

3.3. Global asymptotic stability of DFE: special case

In this section, we explore extending the result in Theorem 3.1 to prove the global asymptotic stability of the DFE for the special case of the model (2.1). Consider the model (2.1) with $\varepsilon_p\,c_p = 1$ and $\delta_u = \delta_d = 0$. Setting $\delta_u = \delta_d = 0$ into the model (2.1),

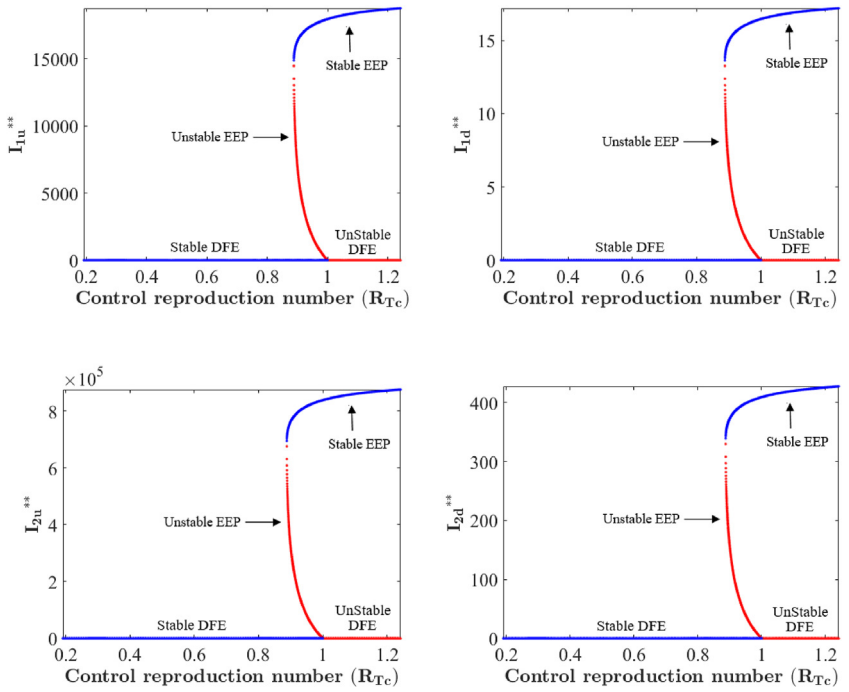

Fig. 3. Backward bifurcation diagram for the model (2.1), showing the profiles of the population of (a) undetected HIV-infected individuals in the primary infection stage of infection (I_{1u}), (b) detected HIV-infected individuals in the primary infection stage of infection (I_{1d}), (c) undetected HIV-infected individuals in the secondary infection stage of infection (I_{2u}) and (d) detected HIV-infected individuals in the secondary infection stage of infection (I_{2d}), as a function of the control reproduction number $\mathbb{R}_{T_c}$. Parameter values used are: $\Pi = 100000$, $p = 0.81$, $\psi_L = 0.99$, $\psi_H = 0.0001$, $\sigma_{1u} = 5.1$, $\sigma_{1d} = 0.1$, $\sigma_{2u} = 0.1$, $\sigma_{2d} = 0.1$, $\xi_d = 0.01$, $\varepsilon_d = 0.01$, $\varepsilon_p = 0.01$, $c_p = 1$, $\eta_d = 0.1$, $\eta_2 = 0.1$, $\eta_A = 0.1$, $\eta_H = 0.009$, $\delta_u = 10.1$, $\delta_d = 0.1$, $\tau_1 = 0.0001$, $\tau_2 = 0.1$, $\tau_A = 0.1$, $\mu = 0.009$ and $\beta = 50$. With this arbitrary set of parameter values, the values of the associated backward bifurcation coefficients (denoted by a and b, and given in (A.7) and (A.8)) are $a = 9.925338500 \times 10^{-5} > 0$ and $b = 0.04638601600 > 0$, respectively. Apart from the efficacies (i.e., ε_d and ε_p), modification parameters (i.e., η_d, η_2, η_A and η_H), the proportion "p'' and the compliance parameter "c_p'', which are dimensionless, all the other parameters have a unit of *per* year (Tollett, 2023).

and adding all the equations, shows that $\frac{dN}{dt} = \Pi - \mu N$, from which it follows that $N(t) \to \frac{\Pi}{\mu}$ as $t \to \infty$. From now on, the total population at time t, $N(t)$, will be replaced by its limiting value, $N^* = \Pi/\mu$. In other words, the standard incidence formulation for the infection rate is now replaced by a mass action incidence. Consider the following feasible region for the special case of the two-group model (2.1) (Tollett, 2023):

$$\Gamma^* = \left\{(S_L, S_H, I_{1_u}, I_{1_d}, I_{2_u}, I_{2_d}, A_u, A_d, T) \in \Gamma : S_L \leq S_L^*, S_H \leq S_H^*\right\}.$$

It can be shown that the region Γ^* is positively-invariant and attracting with respect to this special case of the model (see Appendix B).

The control reproduction number of this special case of the two group model, denoted by $\hat{\mathbb{R}}_{T_c}$, is given by:

$$\hat{\mathbb{R}}_{T_c} = \rho\left(\hat{F}\hat{V}^{-1}\right) = \mathbb{R}_{T_c}|_{\epsilon_p\ c_p=1, \delta_u=\delta_d=0}. \tag{3.13}$$

We claim the following result:

Theorem 3.4. *Consider the special case of the model* (2.1) *with* $\varepsilon_p\ c_p = 1$ *and* $\delta_u = \delta_d = 0$. *The disease-free equilibrium of the special case of the model* (2.1), $\mathcal{E}_{DF}$ *is globally-asymptotically stable in* Γ^* *whenever* $\hat{\mathbb{R}}_{T_c} < 1$.

The proof of Theorem 3.4, based on using a comparison theorem argument (Gumel et al., 2021; Lakshmikantham & Leela, 1969; Safdar et al., 2023), is given in Appendix B. The result of Theorem 3.4 is numerically illustrated in Fig. 4, where all initial conditions of the special case of the model converged to the disease-free equilibrium when the associated control reproduction number, $\hat{\mathbb{R}}_{T_c}$, is less than one. The epidemiological implication of Theorem 3.4 is that, for the special case of the model (2.1) with $\varepsilon_p\ c_p = 1$ and $\delta_u = \delta_d = 0$, the HIV-disease can be eliminated from the State of Arizona if the threshold quantity, $\hat{\mathbb{R}}_{T_c}$, can be brought to (and maintained at) a value less than one. In other words, for the aforementioned special case of the model (2.1), having $\hat{\mathbb{R}}_{T_c} < 1$ is necessary and sufficient for the effective control (or elimination) of HIV in the State of Arizona (Tollett, 2023).

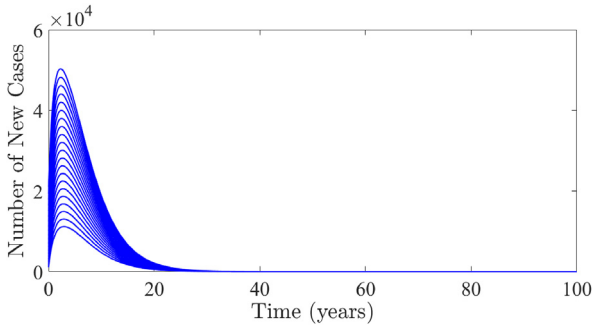

Fig. 4. Simulations of the model (2.1), for the number of new cases as a function of time, showing convergence of initial conditions to the disease-free equilibrium when $\hat{\mathbb{R}}_{T_c} < 1$. Parameter values used are as given in Table 3 with $\beta = 0.25$ (so that, $\hat{\mathbb{R}}_{T_c} = 0.4649 < 1$). For these simulations, the associated backward bifurcation coefficient, a, takes the value $a = -5.41730928 \times 10^{-5} < 0$, and the associated backward bifurcation coefficient, b, takes the value $b = 0.181937418 > 0$ (Tollett, 2023).

It is worth mentioning that substituting $\varepsilon_p\, c_p = 1$ and $\delta_u = \delta_d = 0$ into the expressions for the backward bifurcation coefficients (a and b) in (A.7) and (A.8), and simplifying, shows that $a = -5.41730928 \times 10^{-5} < 0$ and $b = 0.181937418 > 0$. Thus, it follows from Item (i) of Theorem 4.1 in (Castillo-Chavez & Song, 2004) that the special case of the model (2.1) with $\varepsilon_p\, c_p = 1$ and $\delta_u = \delta_d = 0$ will not undergo backward bifurcation at $\hat{\mathbb{R}}_{T_c} = 1$ (this is in line with the global asymptotic stability result proved for the DFE of the special case of the model in Theorem 3.4; as illustrated in Fig. 4, where all initial conditions of the model converged to the DFE when the conditions for the absence of backward bifurcation are achieved) (Tollett, 2023).

4. Global parameter sensitivity analysis

The model (2.1) contains 23 parameters. Although the baseline values of these parameters are available from the literature (as tabulated in Table 3), uncertainties are expected to arise in the estimate of their values (Safdar & Abba, 2023). It is, therefore, crucial to assess the impact of these uncertainties on the outcome of the model simulations (Simpson & Gumel, 2017; Safdar & Abba, 2023; M Blower & Dowlatabadi, 1994; McLeod et al., 2006; Marino et al., 2008). Furthermore, it is also important to identify the key parameters of the model that have the most influence on the dynamics of the model with respect to a chosen response function. In this section, global parameter sensitivity analyses will be carried out to determine the parameters that have the most influence on the chosen response function (i.e., the *control reproduction number* ($\mathbb{R}_{T_c}$)) for the model (2.1). Since the values of two of the parameters of the model (2.1), namely the demographic parameters Π and μ, are reliably known for the target (available from the population health and vital statistics data obtained from the Arizona Department of Health Services (Arizona Department of Health Services, 2023)), they are excluded from the sensitivity analysis to be carried out in this section (i.e., the sensitivity analysis will be based on the remaining 21 parameters of the model (2.1)) (Tollett, 2023).

Global parameter sensitivity analysis is carried out to determine the key parameters of the model (2.1) that have the most influence on the aforementioned response function ($\mathbb{R}_{T_c}$). Partial rank correlation coefficients (PRCCs) is used to determine the parameters of the model that have the most effect on the chosen response function (M Blower & Dowlatabadi, 1994; McLeod et al., 2006; Marino et al., 2008). The parameters with large PRCC values (greater or equal to 0.5 in magnitude) are considered to be the most influential to the response function (Taylor, 1990). The process of carrying out the global parameter sensitivity analysis entails defining a range (lower and upper bound) and distribution for each parameter of the model (2.1), and then splitting each parameter range into 1000 equal sub-intervals. Parameter sets are drawn from this space without replacement and used to form a $1,000 \times 21$ matrix (hypercube). Each row of this matrix is used to compute the response function (i.e., $\mathbb{R}_{T_c}$ in this case) and PRCCs are then computed to assess the contributions of uncertainty and variability in individual parameters to uncertainty and variability in the reproduction number. Parameters with high PRCC values close to -1 or $+1$ are said to be highly correlated with the response function (those with negative (positive) PRCC values are said to be negatively (positively) correlated with the response function). We assume, for simplicity, that each of the 21 parameters of the model (2.1) obeys a uniform distribution, and the range for each parameter is obtained by taking 20% to the left, and then 20% to the right, of its baseline value (given in Table 5). The results of the sensitivity analysis conducted on the model (2.1), with respect to the response function $\mathbb{R}_{T_c}$, are depicted in Fig. 5. It follows from this figure that the top five PRCC-ranked parameters that have the most influence on the response function ($\mathbb{R}_{T_c}$) are (Tollett, 2023):

1. The effective contact rate (β).
2. The modification parameter for the assumed increase in the likelihood of acquiring an HIV infection by high-risk susceptible individuals (η_H).
3. The modification parameter for reduced infectiousness of detected individuals, in relation to undetected individuals (η_d).
4. Transition rate of susceptible individuals from the high-risk to the low-risk susceptible compartment (ψ_H).

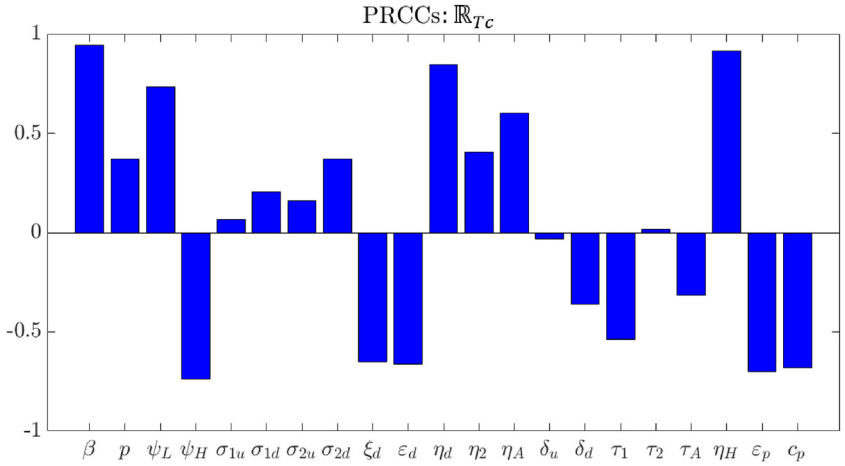

Fig. 5. Partial rank correlation coefficients (PRCCs) depicting the impact of the parameters of the model (2.1) with respect to the response function (or burden of the HIV/AIDS in the MSM community), $\mathbb{R}_{T_c}$. The parameters used in these simulations are as given by the baseline values, and their corresponding ranges are as given in Table 5 (Tollett, 2023).

5. Transition rate of susceptible individuals from the low-risk to the high-risk susceptible compartment (ψ_L).

Therefore, it follows from the global parameter sensitivity analysis that HIV/AIDS can be effectively controlled in the MSM population by implementing intervention and mitigation measures that focus on the following strategies:

(i) Reducing the effective contact rate (i.e., reduce β). This can be achieved by minimizing the number of sexual partners, consistently using condoms during sexual intercourse and avoiding needle-sharing by injection-drug MSM users.
(ii) Reducing the increased likelihood of high-risk susceptible individuals from acquiring an HIV infection, in comparison to low-risk susceptible individuals (i.e., reduce η_H). This can be achieved by encouraging high-risk individuals to get tested frequently to keep them aware of their HIV infection status (and risk), reducing their number of sexual partners, using sterilized needles (by high-risk susceptible injection-drug MSM users), and using condoms consistently during sexual intercourse.
(iii) Reducing the value of the modification parameter for the assumed reduction of infectiousness of detected individuals, in comparison to undetected infectious individuals (i.e., reduce η_d). This can be achieved by encouraging individuals to get tested frequently and to immediately treat the detected infected individuals (in addition to counselling them to desist from risky practices that could lead them to infect their susceptible partners).
(iv) Increasing the transition rate of susceptible individuals from the high-risk to the low-risk susceptible compartment (i.e., increase ψ_H). This can be achieved by the implementation of effective public health education and counselling campaigns, specifically targeting high-risk individuals. These efforts aim to alter their behaviors that elevate the risk of acquiring an HIV infection. In other words, it is crucial to implement strategies that promote positive behavioral shifts, thereby encouraging high-risk individuals to transition towards the low-risk, HIV-susceptible category.
(v) Reducing the increase in risky behavior (i.e., reduce ψ_L). This can be achieved by implementing effective public health education and counselling campaigns that discourage low-risk individuals from engaging in risky behavior that increases their likelihood of acquiring an HIV infection. In other words, effective strategies that encourages positive change of behavior (so that low-risk individuals do not change their behavior and transition to the high-risk HIV-susceptible class) should be implemented.

It should be mentioned that other notable influential parameters (with respect to the response function, but not as influential as the aforementioned top-five) of the model are the efficacy of the diagnostic test to detect undetected individuals (ε_d), the detection rate of diagnostic test administered the compliance in PrEP usage (ξ_d), the efficacy of PrEP to prevent high-risk susceptible individuals from acquiring an HIV infection (ε_p), the compliance in PrEP usage (c_p) and the treatment rate of detected individuals in I_{1d} class (τ_1).

In summary, based on the global parameter sensitivity analysis conducted in this section, this study identifies top-five PRCC ranked parameters of the model (2.1), namely, β, η_H, η_d, ψ_H and ψ_L, that have the greatest influence on the value of the chosen response function of the model (i.e., the control reproduction number, ($\mathbb{R}_{T_c}$), which governs the persistence or effective control of the HIV/AIDS pandemic for the MSM population in the State of Arizona). Hence, in order to effectively curtail the HIV/AIDS epidemic in the MSM population, the control and mitigation interventions implemented in the MSM community should focus on effectively targeting the aforementioned top-five PRCC-ranked parameters.

5. Numerical simulations

The model (2.1) will now be simulated to assess the population-level impact of the effective contact rate, the compliance of PrEP coverage, the duration before detection of undetected individuals, modification parameters (η_d and η_H) and behaviour change on the dynamics of HIV/AIDS in an MSM community in the State of Arizona. Unless otherwise stated, the simulations will be carried out using the baseline values of the parameters as tabulated in Table 5. Furthermore, in the numerical simulations to assess the impact of one intervention, the other interventions are maintained at their baseline values (as given in Table 5).

5.1. Assessing the impact of heterogeneity in effective contact rate

The model (2.1) will now be simulated to assess the community-wide impact of heterogeneity in the effective contact rate on the efficacy of PrEP and compliance of PrEP coverage. Fig. 6 depicts the contour plots of the control reproduction number ($\mathbb{R}_{T_c}$) of the model (2.1), as a function of the efficacy of PrEP (ε_p) and compliance in PrEP usage (c_p). For all the simulations depicted in Fig. 6(a) – (c), all the parameters are maintained at their baseline values, as tabulated in Table 5. It follows from the contour plot depicted in Fig. 6(a) that the value of $\mathbb{R}_{T_c}$ decreases with the increasing efficacy of PrEP and compliance in PrEP usage. Fig. 6(b) further shows that if β is increased by 3-fold from its baseline value (while PrEP efficacy is maintained at its baseline value of 96%, as given in Table 5), at least 47% of the high-risk susceptible MSM population needs to be on PrEP to bring (and maintain) the control reproduction number ($\mathbb{R}_{T_c}$) to a value below one. However, if β is increased by 5-fold from its baseline value (with PrEP efficacy maintained at 96%), then the PrEP compliance needed to bring (and maintain) the control reproduction number to a value below one dramatically increases to 76% (Fig. 6(c)). In summary, the contour plots depicted in Fig. 6 show that, for baseline PrEP efficacy, the level of PrEP compliance needed to bring (and maintain) the control reproduction number to a value less than one increases significantly with increasing the value of the effective contact rate (β) in the MSM community.

5.2. Assessing the effect of compliance of PrEP coverage

The model (2.1) is further simulated to assess the population-level impact of PrEP compliance on the dynamics of HIV in the MSM population. Specifically, simulations are carried out for the yearly and cumulative yearly cases of HIV in the MSM population, as a function of PrEP compliance coverage (c_p), while keeping all the other parameters of the model at their baseline values (tabulated in Table 5). The results obtained are depicted in Fig. 7. In particular, Fig. 7(a) shows a significant decrease in the average yearly new cases recorded at the peak, with increasing coverage in PrEP compliance, as expected (i.e., compare the peaks for the gold and green curves in Fig. 7(a), with the peaks of the blue curve, which represents the baseline scenario). For instance, this figure shows that if the compliance in PrEP usage is increased to 50%, then about 22% of the yearly new HIV/AIDS cases recorded at the peak could have been averted, in comparison to the baseline scenario (i.e., compare the peaks of the blue and gold curves in Fig. 7(a)). Furthermore, if the compliance in PrEP usage is increased to 80%, then about 50% of the yearly new HIV/AIDS cases recorded at the peak could have been averted, in comparison to the baseline scenario (i.e., compare the peaks of the blue and green curves in Fig. 7(a)). On the other hand, for the worst case scenario (i.e., where PrEP-based intervention is not implemented in the MSM community), there is a marked increase in the average yearly new cases recorded at the peak (i.e., compare the peak for the magenta curve in Fig. 7(a), with the peaks of the blue curve, which represents the baseline scenario). For this worst case scenario, about 37% of the new yearly HIV/AIDS cases recorded at the peak increases, in comparison to the baseline scenario (i.e., compare peaks of blue and magenta curves in Fig. 7(a)).

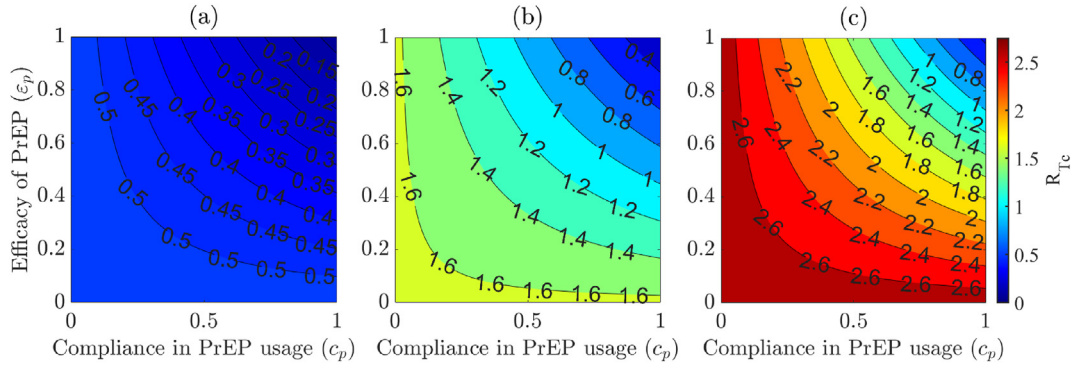

Fig. 6. Contour plots of the control reproduction number ($\mathbb{R}_{T_c}$) of the model (2.1), as a function of the efficacy of PrEP (ε_p) and compliance in PrEP usage (c_p). (a) The effective contact rate (β) kept at its baseline. (b) The effective contact rate (β) increased by 3-fold from its baseline value. (c) The effective contact rate (β) increased by 5-fold from its baseline value. Other parameter values used in the simulations are as given by their baseline values in Table 5.

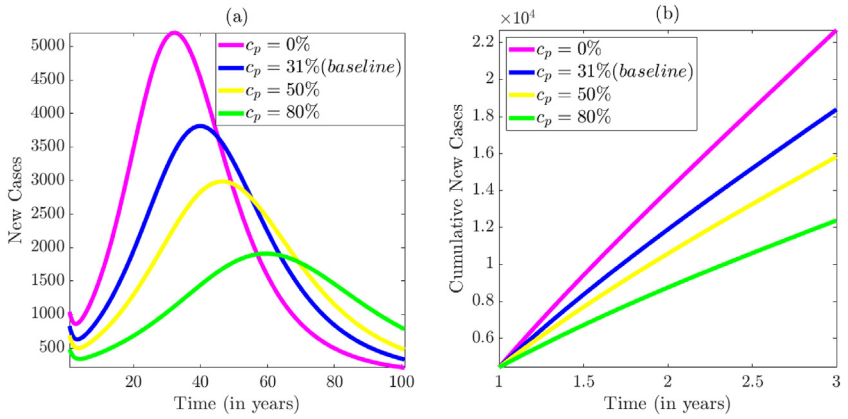

Fig. 7. Simulations of the model (2.1), showing (a) new cases of HIV/AIDS and (b) cumulative new cases of HIV/AIDS in the MSM population in the State of Arizona, as a function of time, for various values of the compliance in PrEP usage (c_p). Values of the other parameters of the model (2.1) used in these simulations are as given by their respective baseline values tabulated in Table 5.

Similar dynamics are observed with respect to the cumulative number of yearly new cases, for the aforementioned levels of compliance of PrEP coverage considered in these simulations, in comparison to the baseline scenario (as illustrated in Fig. 7(b)).In summary, the simulations in this section show that increasing (decreasing) PrEP coverage in the high-risk susceptible MSM population resulted in a marked reduction (increase) in the average number of new (and cumulative) yearly cases recorded at the peak, in comparison to the baseline scenario.

5.3. Assessing the effect of duration before detection of undetected individuals

The model (2.1) is now simulated to assess the effect of the average duration before the detection of undetected infectious individuals ($1/\xi_d$) and the efficacy of the diagnostic test (ε_d) on the dynamics of HIV/AIDS in the MSM community in the State of Arizona. The simulations are carried out using the baseline values of the other parameters of the model, tabulated in Table 5. The results obtained, depicted by the contour plot of the control reproduction number of the model, as a function of $1/\xi_d$ and ε_d (in Fig. 8), show that regardless of the values of the efficacy of the diagnostic test, early detection of undetected infectious individuals significantly reduces the control reproduction number (hence, reduce the disease burden). Thus, it can be concluded from Fig. 8 that, for the baseline value of the efficacy of diagnostic test to detect undetected individuals (i.e., $\varepsilon_d = 1.5$), the control reproduction number can be brought to a value below one if (on average) undetected infected individuals can be detected within about 6 years, and the corresponding value of the detection rate of diagnostic test administered is 0.161 (i.e., $\xi_d = 0.161$).

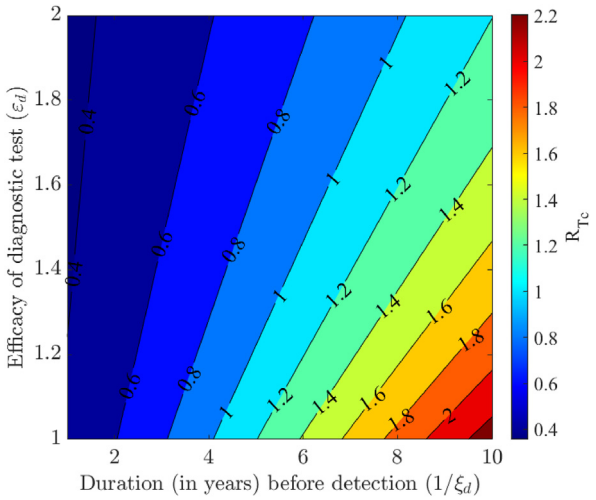

Fig. 8. Contour plot of the control reproduction number ($\mathbb{R}_{T_c}$) of the model (2.1), as a function of efficacy of diagnostic test to detect undetected individuals (ε_d) and the duration before detection ($1/\xi_d$). Parameter values used are as given by their baseline values in Table 5.

5.4. Assessing the effect of modification parameters (η_d and η_H)

The combined impacts of the modification parameters for reduced infectiousness of detected individuals, in relation to undetected individuals (η_d) and the modification parameter for the assumed increase in the likelihood of acquiring an HIV infection by high-risk susceptible individuals (η_H) is monitored by simulating the model (2.1) using the baseline parameters in Table 5. The results obtained, depicted by the contour plots in Fig. 9, show a significant decrease in the value of the control reproduction number ($\mathbb{R}_{T_c}$) with decreasing values of the modification parameter η_H (where the reproduction number decreases from 1.8 to 0.4, as η_H decreases from 4.3 to 3.8), regardless of the values of the modification parameter for reduced infectiousness of detected individuals, in relation to undetected individuals (η_d). Thus, it can be concluded that, for the baseline value of the modification parameter for the reduced infectiousness of detected individuals, in relation to undetected individuals (i.e., $\eta_d = 0.43$), the value of the modification parameter for the assumed increase in the likelihood of acquiring an HIV infection by high-risk susceptible individuals need to be 4.15 or less in order to reduce the control reproduction number ($\mathbb{R}_{T_c}$) below one (i.e., for this setting, high-risk susceptible individuals should not be more than 15% more likely to acquire HIV infection, in comparison to their low-risk counterparts).

5.5. Assessing the effect of behaviour change

The model (2.1) is further simulated to assess the effect of negative behavior change (from low-risk to high-risk susceptible population) and positive behavior change (from high-risk to low-risk susceptible population) on the dynamics of HIV/AIDS in the MSM community. The simulations are carried out using the baseline values of the parameters of the model (tabulated in Table 5). Fig. 10 depict the contour plots of the control reproduction number of the model (2.1), as a function of the transition rate from low-risk to high-risk susceptible population (ψ_L) and the transition rate from high-risk to low-risk susceptible population (ψ_H). It follows from the contour plots depicted in Fig. 10(a) that the value of the control reproduction number ($\mathbb{R}_{T_c}$) decreases with the decreasing values of the transition rate from low-risk to high-risk susceptible population and with the increasing values of the transition rate from high-risk to low-risk susceptible population. Furthermore, our simulations show that if the transmission rate β is increased by 3-fold from its baseline value, and the value of ψ_L is kept at baseline, then the value of ψ_H needs to be at least 0.90 *per* year (i.e., if the duration before the transition of susceptible individuals from high-risk to low-risk susceptible population is at most 1.1 years), to bring the control reproduction number ($\mathbb{R}_{T_c}$) below one (Fig. 10(b)). However, if β is increased by 5-fold from its baseline value then the transition rate of susceptible individuals from low-risk to high-risk susceptible population (ψ_L) needs to be below 0.141 *per* year (regardless of the value of the transition rate from high-risk to low-risk susceptible population) to bring the control reproduction number below unity (Fig. 10(c)). In other words, the prospects of eliminating HIV/AIDS in the MSM population is promising if the duration before the transition of susceptible individuals from low-risk to high-risk susceptible population is at least 8 years (i.e., if low-risk individuals take at least 8 years before they change their risky behavior and transition to the high-risk group). In summary, it follows from the results depicted in Fig. 10 that the value of the control reproduction number ($\mathbb{R}_{T_c}$) decreases significantly with increasing values of the transition rate from high-risk to low-risk susceptible population (ψ_H) even if the effective contact rate (β) is increasing. Furthermore, if the effective contact rate (β) is increased by 5-fold from its baseline value, then the value of the

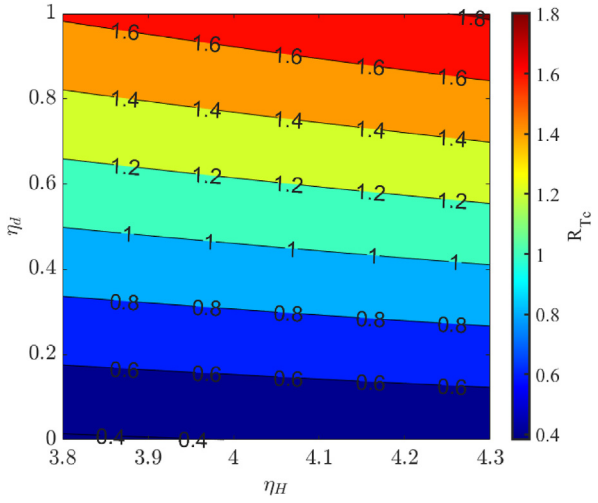

Fig. 9. Contour plot of the control reproduction number ($\mathbb{R}_{T_c}$) of the model (2.1), as a function of the modification parameter for the assumed reduction in the infectiousness of detected individuals, in relation to undetected individuals (η_d) and the modification parameter for the assumed increase in the likelihood of acquiring an HIV infection by high-risk susceptible individuals (η_H). Parameter values used are as given by their baseline values in Table 5.

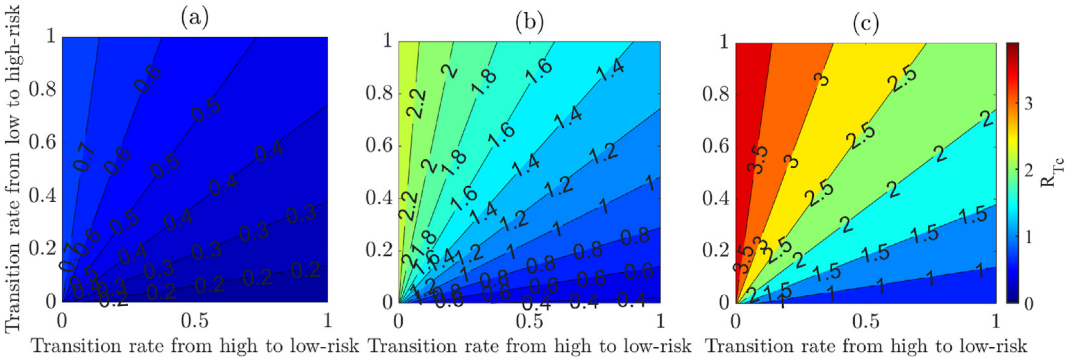

Fig. 10. Contour plot of the control reproduction number ($\mathbb{R}_{T_c}$) of the model (2.1), as a function of the transition rate from low-risk to high-risk susceptible population (ψ_L) and the transition rate from high-risk to low-risk susceptible population (ψ_H) when (a) the effective contact rate (β) is at the baseline, (b) the effective contact rate (β) is increased by 3-fold from the baseline value, (c) the effective contact rate (β) is increased by 5-fold from the baseline value. The units of ψ_L and ψ_H are *per* year. The other parameter values used are as given by their baseline values in Table 5.

transition rate from low-risk to high-risk susceptible population (ψ_L) must be reduced significantly to have any realistic chance for the effective control or elimination of the disease in the MSM community.

6. Discussion and conclusions

This study is based on the use of mathematical modeling approaches to assess the combined impacts of risk-structure and the use of pre-exposure prophylaxis (PrEP) on the spread and control of HIV/AIDS in a sexually-active MSM population in the State of Arizona. Specifically, a novel two-group model (low-risk and high-risk), which takes the form of a 9-dimensional deterministic system of nonlinear differential equations is developed. This model, which extends numerous other HIV transmission models in the literature, was rigorously analyzed to gain insight into its qualitative features. The analyses revealed that the disease-free equilibrium of the model is locally-asymptotically stable whenever the associated control reproduction number of the model (denoted by $\mathbb{R}_{T_c}$) is less than one. Using the theory of center manifold, it was shown that the model undergoes the dynamic phenomenon of backward bifurcation when the associated reproduction number ($\mathbb{R}_{T_c}$) is less than unity under certain conditions. The epidemiological implication of the backward bifurcation phenomenon is that the usual epidemiological requirement of having the control reproduction number of the model being less than unity, while necessary, is no longer sufficient for the elimination of the disease in the community. Furthermore, when the phenomenon of backward bifurcation occurs, more control measures need to be implemented to further reduce the control reproduction number. A sufficient condition for the presence of backward bifurcation in the model was identified, namely the imperfect nature of the efficacy and compliance of PrEP in the MSM community. The disease-free equilibrium for the special case of the model with perfect PrEP efficacy and compliance, and no disease-induced mortality (i.e., by setting $\varepsilon_p c_p = 1$ and $\delta_u = \delta_d = 0$ in the two-group model), where backward bifurcation does not occur, is shown to be globally-asymptotically stable when the associated control reproduction number of the model is less than one. The epidemiological implication of this global asymptotic stability result for the special case of the model is that the HIV/AIDS pandemic can be eliminated from the MSM community in the State of Arizona if the control measures implemented can bring (and maintain) the associated reproduction number to a value less than one. The HIV/AIDS pandemic will persist in the MSM community if the control measures implemented are unable to bring (and maintain) the control reproduction number to a value less than one. Furthermore, the model was parameterized by fitting it to the observed yearly new HIV case data for an MSM community in the State of Arizona for the period 1990–2019.

Using global sensitivity analysis of the model, we identified the parameters of the model that have the most influence on the control reproduction number of the model, $\mathbb{R}_{T_c}$. Specifically, the top-five PRCC ranked parameters that had the most impact on the control reproduction number are; the effective contact rate (β), the modification parameter for the assumed increase in the likelihood of acquiring an HIV infection by high-risk susceptible individuals (η_H), the modification parameter for reduced infectiousness of detected individuals, in relation to undetected individuals (η_d), the transition rate from high-risk to low-risk susceptible population (ψ_H) and the transition rate from low-risk to high-risk susceptible population (ψ_L). The numerical PRCC values indicate that reduction of β, η_H, η_d and ψ_L, and increasing ψ_H, results in the reduction of $\mathbb{R}_{T_c}$. The parameter β can be reduced by minimizing the number of sexual partners, consistently using condoms during sexual intercourse and avoiding injection-drug by MSM users. The parameter η_H can be reduced by encouraging high-risk susceptible individuals to get tested frequently to keep them aware about their HIV-infection status (and risk), using sterilized needles (by high-risk susceptible injection-drug MSM users), using condoms consistently during sexual intercourse and reducing the number of sexual partners. The parameter ψ_L can be reduced by a change of behaviour *via* public health education campaigns to give awareness about the consequences of unsafe sexual intercourse and the effects of sharing needles (in other word, by promoting counselling campaigns that discourage low-risk individuals from engaging in risky behavior). Furthermore, by

decreasing the value of the modification parameter for reduced infectiousness of detected individuals (i.e., by encouraging individuals to get tested frequently and to immediately treat the detected infected individuals) and by increasing the parameter ψ_H (*via* public health education campaigns, to promote awareness about the risks associated with unprotected sexual intercourse and the high risks associated with needle-sharing), will ultimately reduce $\mathbb{R}_{T_c}$.

We carried out extensive numerical simulations to assess the impact of heterogeneity in effective contact rate and the efficacy of PrEP and compliance in PrEP usage on the dynamics of HIV/AIDS disease in the MSM community of the State of Arizona. These simulations showed, as expected, that the control reproduction number ($\mathbb{R}_{T_c}$) decreases significantly with the increasing efficacy of PrEP and compliance in PrEP usage (while all other parameters are maintained at their baseline values), even if the effective contact rate is increasing. For instance, if the effective contact rate (β) is increased by 3-fold from its baseline value for the efficacy of PrEP set at about 96%, at least 47% of the compliance in PrEP usage is needed to bring the control reproduction number ($\mathbb{R}_{T_c}$) below one. However, if β is increased by 5-fold from its baseline value for the efficacy of PrEP set at about 96% then the compliance in PrEP usage drastically increases to 76% to bring the control reproduction number below unity. Furthermore, we also simulated the model to assess the effect of compliance of PrEP coverage on the peak yearly new cases. The numerical simulations showed a marked decrease in the average yearly new cases recorded at the peak when the compliance in PrEP coverage is increased (while other interventions are maintained at their baseline values), in comparison to the corresponding scenario when no PrEP compliance is implemented. Specifically, for the scenario when the compliance in PrEP usage is 50%(80%) then about 22%(50%) of the yearly new HIV/AIDS cases recorded at the peak will have been prevented, in comparison to the baseline scenario. On the other hand, if there is no compliance in PrEP usage (i.e., for the worst case scenario) then the increase in the yearly new HIV/AIDS cases recorded at the peak is about 37%, in comparison to the baseline scenario. Our simulations also showed that the control reproduction number can be brought to a value below one if (on average) undetected infected individuals can be detected and treated within about 6 years (while all other interventions are maintained at their baseline levels). Furthermore, this study also showed that, for the baseline value of the modification parameter for the reduced infectiousness of detected individuals, in relation to undetected individuals, the prospects of HIV/AIDS pandemic elimination in the MSM community is possible if high-risk susceptible individuals should not be more than 15% more likely to acquire HIV infection, in comparison to their low-risk counterparts.

This study also addressed an important question related to the community-wide impact of behaviour change (i.e., negative or positive behaviour change) in the MSM population on the dynamics of HIV/AIDS pandemic in the State of Arizona (specifically, the duration before the transition of the susceptible individuals from high-risk to low-risk susceptible population or vice versa). The numerical simulations showed that the value of the control reproduction number ($\mathbb{R}_{T_c}$) decreases (increases) significantly with the decreasing (increasing) values of transition rate from low-risk to high-risk susceptible population (ψ_L) even if the effective contact rate (β) has increased up to 5-fold from its baseline value (while all other interventions are maintained at their baseline values). It was also shown that for the scenario when the effective contact rate is increased by 3-fold from its baseline value and the value of the transition rate from low-risk to high-risk susceptible population is kept at the baseline value then for the HIV pandemic elimination, the duration before the transition of susceptible individuals from high-risk to low-risk susceptible population needs be at most 1.1 years. Furthermore, if the effective contact rate (β) is increased by 5-fold from its baseline value then low-risk individuals take at least 8 years before they change their risky behavior and transition to the high-risk group (regardless of the value of the transition rate from high-risk to low-risk susceptible population), in order to eliminate the HIV/AIDS disease from the MSM community.

Some of the limitations of the two group model presented in this study include not incorporating different detection rates of diagnostic test administered for the HIV-infected individuals in the primary, secondary and AIDS stage of infection. This study also assumes that the efficacy of the diagnostic test implemented is same in all undetected infected compartments. Furthermore, the model does not incorporate the condom use strategy (which remains the most effective HIV prevention strategy) along with the use of pre-exposure prophylaxis (PrEP) on the spread and control of HIV/AIDS in an MSM population.

CRediT authorship contribution statement

Queen Tollett: Conceptualization, Data curation, Formal analysis, Methodology, Validation, Visualization, Writing – original draft, Writing – review & editing. **Salman Safdar:** Data curation, Formal analysis, Validation, Visualization, Writing – review & editing. **Abba B. Gumel:** Conceptualization, Funding acquisition, Methodology, Project administration, Supervision, Writing – original draft, Writing – review & editing.

Declaration of competing interest

None.

Acknowledgments

ABG acknowledges the support, in part, of the National Science Foundation (Grant Number: DMS-2052363; transferred to DMS-2330801). SS acknowledges the support of the Fulbright Foreign Student Program. The authors are grateful to the anonymous reviewers for their constructive comments.

Appendix A. Proof of Theorem 3.3

proof. The proof is based on the center manifold theory (van den Driessche & James, 2002; Carr, 2012). To apply this theory, it is convenient, first of all, to let $S_L = x_1$, $S_H = x_2$, $I_{1_u} = x_3$, $I_{1_d} = x_4$, $I_{2_u} = x_5$, $I_{2_d} = x_6$, $A_u = x_7$, $A_d = x_8$ and $T = x_9$. The model (2.1) can be re-written in the general form (by using the aforementioned transformation of variables); $\frac{dX}{dt} = (f_1, f_2, f_3, f_4, f_5, f_6, f_7, f_8, f_9)^T$, with $X = (x_1, x_2, x_3, x_4, x_5, x_6, x_7, x_8, x_9)^T$. Specifically, the model (2.1) can be written in terms of the transformed variables as:

$$\begin{cases} \frac{d x_1}{d t} = f_1 = & \Pi(1-p) + \psi_H x_2 - \lambda x_1 - k_1 x_1, \\ \frac{d x_2}{d t} = f_2 = & \Pi p + \psi_L x_1 - \eta_H(1-\epsilon_p c_p)\lambda x_2 - k_2 x_2, \\ \frac{d x_3}{d t} = f_3 = & \lambda x_1 + \eta_H(1-\epsilon_p c_p)\lambda x_2 - k_3 x_3, \\ \frac{d x_4}{d t} = f_4 = & \epsilon_d \xi_d x_3 - k_4 x_4, \\ \frac{d x_5}{d t} = f_5 = & \sigma_{1u} x_3 - k_5 x_5, \\ \frac{d x_6}{d t} = f_6 = & \epsilon_d \xi_d x_5 + \sigma_{1d} x_4 - k_6 x_6, \\ \frac{d x_7}{d t} = f_7 = & \sigma_{2u} x_5 - k_7 x_7, \\ \frac{d x_8}{d t} = f_8 = & \sigma_{2d} x_6 + \epsilon_d \xi_d x_7 - k_8 x_8, \\ \frac{d x_9}{d t} = f_9 = & \tau_I x_4 + \tau_2 x_6 + \tau_A x_8 - k_9 x_9, \end{cases} \tag{A.1}$$

where,

$$\begin{aligned} \lambda \quad &= \beta\left[\frac{x_3 + \eta_d x_4 + \eta_2(x_5 + \eta_d x_6) + \eta_A(x_7 + \eta_d x_8)}{N}\right], k_1 = \psi_L + \mu, k_2 = \psi_H + \mu, k_3 = \epsilon_d\ \xi_d + \sigma_{1u} + \mu, \\ & k_4 = \tau_1 + \sigma_{1d} + \mu, k_5 = \epsilon_d\ \xi_d + \sigma_{2u} + \mu, k_6 = \tau_2 + \sigma_{2d} + \mu, \\ & k_7 = \epsilon_d\ \xi_d + \mu + \delta_u, k_8 = \tau_A + \mu + \delta_d, k_9 = \mu. \end{aligned} \tag{A.2}$$

Evaluating the Jacobian of the transformed system (A.1) at the DFE ($\mathcal{E}_{DF}$), is given by:

$$J(\mathcal{E}_{DF}) = \begin{pmatrix} -k_1 & \psi_H & -J_1 & -\eta_d J_1 & -\eta_2 J_1 & -\eta_2\ \eta_d J_1 & -\eta_A J_1 & -\eta_A\ \eta_d J_1 & 0 \\ \psi_L & -k_2 & J_2 & -\eta_d J_2 & -\eta_2 J_2 & -\eta_2\ \eta_d J_2 & -\eta_A J_2 & -\eta_A\ \eta_d J_2 & 0 \\ 0 & 0 & J_3 - k_3 & \eta_d J_3 & \eta_2 J_3 & \eta_2\ \eta_d J_3 & \eta_A J_3 & \eta_A\ \eta_d J_3 & 0 \\ 0 & 0 & \xi_d\ \epsilon_d & -k_4 & 0 & 0 & 0 & 0 & 0 \\ 0 & 0 & \sigma_{1_u} & 0 & -k_5 & 0 & 0 & 0 & 0 \\ 0 & 0 & 0 & \sigma_{1_d} & \xi_d\ \epsilon_d & -k_6 & 0 & 0 & 0 \\ 0 & 0 & 0 & 0 & \sigma_{2_u} & 0 & -k_7 & 0 & 0 \\ 0 & 0 & 0 & 0 & 0 & \sigma_{2_d} & \xi_d\ \epsilon_d & -k_8 & 0 \\ 0 & 0 & 0 & \tau_1 & 0 & \tau_2 & 0 & \tau_A & -k_9 \end{pmatrix}, \text{where,}$$

$J_1 = \frac{\beta\{(1-p)\mu + \psi_H\}}{\mu + \psi_H + \psi_L}$, $J_2 = \frac{\beta\ \eta_H(1-\epsilon_p c_p)(\mu p + \psi_L)}{\mu + \psi_H + \psi_L}$ and $J_3 = J_1 + J_2$.

Consider the case when $\mathbb{R}_{T_c} = 1$ and choosing β as the bifurcation parameter, and solving for β when $\mathbb{R}_{T_c} = 1$ (i.e., at the bifurcation point) gives:

$$\beta = \frac{C_1\ C_2\ C_3\ C_4\ C_5\ C_6\ N^*}{B^*\{T_1 + T_2 + T_3 + T_4 + T_5 + T_6\}} = \beta^*,$$

where,

$B^* = S_L^* + \eta_H(1-\epsilon_p c_p)S_H^*$, $N^* = \frac{\Pi}{\mu}$, $T_1 = C_2\, C_3\, C_4\, C_5\, C_6$, $T_2 = C_3\, C_4\, C_5\, C_6\, \eta_d\, \epsilon_d\, \xi_d$, $T_3 = C_2\, C_4\, C_5\, C_6\, \eta_2\, \sigma_{1_u}$, $T_4 = C_5\, C_6\, \eta_2\, \eta_d\, \epsilon_d\, \xi_d\, (C_3\, \sigma_{1_d} + C_2\, \sigma_{1_u})$, $T_5 = C_2\, C_4\, C_6\, \eta_A\, \sigma_{1_u}\, \sigma_{2_u}$, $T_6 = \eta_A\, \eta_d\, \epsilon_d\, \xi_d\, (C_2\, C_4\, \sigma_{1_u}\, \sigma_{1_d} + C_3\, C_5\, \sigma_{1_d}\, \sigma_{2_d} + C_2\, C_5\, \sigma_{1_u}\, \sigma_{2_d})$, and C_1, C_2, C_3, C_4, C_5, C_6 are as defined in (3.2).

Let J_{β^*} denotes the Jacobian of the system (A.1) evaluated at the DFE ($\mathcal{E}_{DF}$). It can be seen that the system (A.1), with $\beta = \beta^*$, has a simple eigenvalue with zero real part and all other eigenvalues having negative real part (Blayneh et al., 2010). Hence, the center manifold theory (Carr, 2012; Castillo-Chavez & Song, 2004) can be applied to analyze the dynamics of the model (2.1) near the bifurcation point (where $\beta = \beta^*$). To apply the theory (in particular, the approach in (Castillo-Chavez & Song, 2004)), the following computations (associated with the left and right eigenvectors of J_{β^*}, corresponding to the zero eigenvalue) are necessary.

Computation of left and right eigenvectors of J_{β^*}

It can be seen that the left eigenvector of J_{β^*}, corresponding to the zero eigenvalue, is given by: $\mathbf{v} = [v_1, v_2, v_3, v_4, v_5, v_6, v_7, v_8, v_9]$, where (noting that J_1, J_2 and J_3 are defined above),

$$\begin{aligned} v_1 &> 0\ (free),\ v_2 = \frac{\psi_H\, v_1}{k_2},\quad v_3 > 0\ (\text{free}),\quad v_9 = 0, v_8 = \frac{\beta\, \eta_A\, \eta_d(-J_1\, v_1 - J_2\, v_2 + J_3\, v_3)}{k_8}, \\ v_6 &= \frac{\beta\, \eta_A\, \eta_d(-J_1\, v_1 - J_2\, v_2 + J_3\, v_3) + \sigma_{2_d}\, v_8}{k_6},\quad v_7 = \frac{\beta\, \eta_A\, (-J_1\, v_1 - J_2\, v_2 + J_3\, v_3) + \epsilon_d\, \xi_d\, v_8}{k_7}, \\ v_4 &= \frac{\beta\, \eta_d(-J_1\, v_1 - J_2\, v_2 + J_3\, v_3) + \sigma_{1_d}\, v_6}{k_4},\quad v_5 = \frac{\beta\, \eta_d(-J_1\, v_1 - J_2\, v_2 + J_3\, v_3) + \sigma_{1_d}\, v_6 + \sigma_{2_u}\, v_7}{k_5}. \end{aligned} \tag{A.3}$$

Furthermore, the right eigenvector of J_{β^*}, corresponding to the zero eigenvalue, is given by:$\mathbf{w} = [w_1,\ w_2,\ w_3,\ w_4,\ w_5,\ w_6,\ w_7,\ w_8,\ w_9]^T$, where,

$$\begin{aligned} w_1 &= \frac{-\beta\, J_1\, (w_3 + \eta_d\, w_4 + \eta_2\, w_5 + \eta_2\, \eta_d\, w_6 + \eta_A\, w_7 + \eta_A\, \eta_d w_8) + \psi_H w_2}{k_1},\quad w_2 > 0\ (\text{free}), \\ w_3 &> 0\ (\text{free}),\quad w_4 = \frac{\epsilon_d\, \xi_d\, w_3}{k_4},\quad w_5 = \frac{\sigma_{1_u}\, w_3}{k_5}, w_7 = \frac{\sigma_{2_u}\, w_5}{k_7}, \\ w_6 &= \frac{\sigma_{1_d}\, w_4 + \epsilon_d\, \xi_d\, w_5}{k_6}, w_8 = \frac{\sigma_{2_d}\, w_6 + \epsilon_d\, \xi_d\, w_7}{k_8}, w_9 = \frac{\tau_1\, w_4 + \tau_2\, w_6 + \tau_A\, w_8}{k_9}. \end{aligned} \tag{A.4}$$

For computational convenience, we set, without loss of generality, the components of the left eigenvectors v_1 and v_3 in (A.3) to one. Similarly, we set the components w_2 and w_3, of the right eigenvector, given in (A.4) to unity.

Computation of backward bifurcation coefficients, a and b

The local bifurcation analysis near the bifurcation point ($\beta = \beta^*$) is determined by the signs of two bifurcation coefficients, denoted by a and b (Carr, 2012; Castillo-Chavez & Song, 2004). Following (Castillo-Chavez & Song, 2004), the expressions for these bifurcation coefficients are, respectively, given by:

$$a = \sum_{k,i,j=1}^{n} v_k w_i w_j \frac{\partial^2 f_k}{\partial x_i \partial x_j}(\mathcal{E}_{DF}, \beta^*), \tag{A.5}$$

and,

$$b = \sum_{k,i=1}^{n} v_k w_i \frac{\partial^2 f_k}{\partial x_i \partial \beta}(\mathcal{E}_{DF}, \beta^*). \tag{A.6}$$

It can be shown, by substituting the expressions for the eigenvectors (w_k and v_k; $k = 1, \ldots, 9$) given in (A.3) and (A.4) and the partial derivatives of the functions f_k ($k = 1, \ldots, 9$) defined in (A.1) into the expressions (A.5) and (A.6), that the bifurcation coefficients now become:

$$a = \frac{1}{\Pi\ (\mu + \psi_H + \psi_L)}[2\ \mu\ \beta\ (C)\ \{(P + Q + R) - (S + T + U)\}], \tag{A.7}$$

and,

$$b = \frac{C\ (X - Y)}{\mu + \psi_H + \psi_L}, \tag{A.8}$$

where,

$$\begin{gathered}
C = w_3 + \eta_d\, w_4 + \eta_2\, w_5 + \eta_2\, \eta_d\, w_6 + \eta_A\, w_7 + \eta_A\, \eta_d\, w_8, \\
P = v_1(w_2\, \mu + w_3\, \mu + w_4\, \mu + w_5\, \mu + w_6\, \mu + w_7\, \mu + w_8\, \mu + w_9\, \mu + w_2\, \psi_H + w_3\, \psi_H + w_4\, \psi_H + w_5\, \psi_H + w_6\, \psi_H \\
+ w_7\, \psi_H + w_8\, \psi_H + w_9\, \psi_H + w_9\, \psi_H + w_2 \psi_H + w_7\, \mu + w_9\, \mu), \\
Q = v_2\, \eta_H\, (1 - \epsilon_p\, c_p)(w_1\, \mu\, p + w_2\, \mu\, p + w_3\, \mu\, p + w_4\, \mu\, p + w_5\, \mu\, p + w_6\, \mu\, p + w_7\, \mu\, p + w_8\, \mu\, p + w_9\, \mu\, p + w_1\, \psi_L \\
+ w_3\, \psi_L + w_4\, \psi_L + w_5\, \psi_L + w_6\, \psi_L + w_7\, \psi_L + w_8\, \psi_L + w_9\, \psi_L), \\
R = v_3\{\, \eta_H\, (1 - \epsilon_p\, c_p)(w_2\, \psi_H + w_2\, \mu) + w_1\, \mu\, p + w_2\, \mu\, p + w_3\, \mu\, p + w_4\, \mu\, p + w_5\, \mu\, p + w_6\, \mu\, p + w_7\, \mu\, p + w_8\, \mu\, p \\
+ w_9\, \mu\, p\}, \\
S = v_1\, \mu\, p\, (w_1 + w_2 + w_3 + w_4 + w_5 + w_6 + w_7 + w_8 + w_9) + v_1\, w_1\, \psi_L, \quad T = v_2\, w_2\, \eta_H\, (1 - \epsilon_p\, c_p)(\psi_H + \mu), \\
U = v_3\, [\{\eta_H\, (1 - \epsilon_p\, c_p)\, (w_1 + w_2 + w_3 + w_4 + w_5 + w_6 + w_7 + w_8 + w_9)\, (\mu\, p + \psi_L)\}] \\
+ \{(w_2 + w_3 + w_4 + w_5 + w_6 + w_7 + w_8 + w_9)(\mu + \psi_H)\}], \\
X = [\{\eta_H\, (1 - \epsilon_p\, c_p)\, v_3(\mu\, p + \psi_L)\}] + v_1\, \mu\, p + v_3\, (\psi_H + \mu)], \; Y = [\{\eta_H\, (1 - \epsilon_p\, c_p)\, v_2(\mu\, p + \psi_L)\}] + v_3 \mu\, p + v_1\, (\psi_H + \mu)].
\end{gathered} \tag{A.9}$$

It follows from Item (i) of Theorem 4.1 of (Castillo-Chavez & Song, 2004) that the model (2.1) will undergo a backward bifurcation at $\mathbb{R}_{T_c} = 1$ whenever the bifurcation coefficients, a and b (given by (A.7) and (A.8), respectively), are positive. It can be shown that the bifurcation coefficient b is automatically positive as follows. First of all, using the definitions for X and Y in (A.9), the quantity $X - Y$ can be simplified to:

$$X - Y = \eta_H\, (1 - \epsilon_p\, c_p)\, (\mu\, p + \psi_L)(1 - v_2), \tag{A.10}$$

which is positive since $\eta_H > 0$, $0 < \varepsilon_p\, c_p < 1$, $\mu > 0$, $p > 0$, $\psi_L > 0$ and the eigenvector $0 < v_2 < 1$ (from (A.3)). Since $X - Y > 0$, $\mu > 0$, $\psi_H > 0$, $\psi_L > 0$ and $C > 0$, it follows from (A.8) that the bifurcation coefficient b is automatically positive. Hence, since the bifurcation coefficient b is always positive, we only need to show that the coefficient a is positive for backward bifurcation to occur. In particular, it can be shown from Equation (A.7), and noting the definitions in (A.9) and the expressions for the eigenvectors in (A.3) and (A.4), that the backward bifurcation coefficient a is positive provided the following inequality holds:

$$P + Q + R > S + T + U. \tag{A.11}$$

Thus, it follows from Item (i) of Theorem 4.1 of (Castillo-Chavez & Song, 2004)), that the model (2.1) will undergo a backward bifurcation at $\mathbb{R}_{T_c} = 1$ whenever inequality (A.11) holds. □

Appendix B Proof of Theorem 3.4

Proof. Before proving the result of Theorem 3.4, it is necessary to establish the following intermediate results.

*B.1 Proof of positive invariance and attractivity of Γ**

Since $N(t) \leq \Pi/\mu$ for all t in Γ^*, it follows from the first equation of the two-group HIV model (2.1) that:

$$\begin{aligned}\frac{dS_L}{dt} &\leq \Pi(1-p)+\left(\frac{\Pi}{\mu}-S_L\right)\psi_H-(\psi_L+\mu)S_L,\\ &\leq \Pi(1-p)+\left(\frac{\Pi}{\mu}\right)\psi_H-(\psi_H+\psi_L+\mu)S_L,\\ &\leq \frac{\Pi}{\mu}\{\mu(1-p)+\psi_H\}-(\psi_H+\psi_L+\mu)S_L,\\ &\leq (\psi_H+\psi_L+\mu)(S_L^*-S_L).\end{aligned}$$

Hence, if $S_L(t)>S_L^*$, then $\frac{dS_L}{dt}$ is negative. Thus, $S_L(t)\leq S_L^*$ for all t, provided that $S_L(0)\leq S_L^*$. Using similar approach for the second equation of the model (2.1), and using the above bound, we get the following bound:

$$\begin{aligned}\frac{dS_H}{dt} &\leq \Pi\ p+\left(\frac{\Pi}{\mu}-S_H\right)\psi_L-(\psi_H+\mu)S_H,\\ &\leq \Pi\ p+\left(\frac{\Pi}{\mu}\right)\psi_L-(\psi_H+\psi_L+\mu)S_H,\\ &\leq (\psi_H+\psi_L+\mu)(S_H^*-S_H).\end{aligned}$$

Similarly, we have $S_H(t)\leq S_H^*$ for all t, provided that $S_H(0)\leq S_H^*$. It follows from these bounds that:

$$\Gamma^*=\left\{\left(S_L(t),S_H(t),I_{1u}(t),I_{1d}(t),I_{2u}(t),I_{2d}(t),A_u(t),A_d(t),T(t)\right)\in\Gamma : S_L\leq S_L^*, S_H\leq S_H^*\right\}, \tag{B.1}$$

is positively-invariant and attracts all initial solutions in Γ*.

B.2 Next generation matrices for the special case of the model (2.1)

For the special case of the model (2.1), the associated next generation matrix of new infection terms, denoted by $\hat{F}$, and the associated next generation matrix of linear transition terms, denoted by $\widehat{V}$, are given as:

$$\widehat{F}=\begin{bmatrix}\frac{\beta S_L^*}{N^*} & \eta_d\frac{\beta S_L^*}{N^*} & \eta_2\frac{\beta S_L^*}{N^*} & \eta_2\eta_d\frac{\beta S_L^*}{N^*} & \eta_A\frac{\beta S_L^*}{N^*} & \eta_A\eta_d\frac{\beta S_L^*}{N^*}\\ 0&0&0&0&0&0\\ 0&0&0&0&0&0\\ 0&0&0&0&0&0\\ 0&0&0&0&0&0\\ 0&0&0&0&0&0\end{bmatrix}$$

and,

$$\widehat{V}=\begin{bmatrix}\widehat{C_1} & 0 & 0 & 0 & 0 & 0\\ -\epsilon_d\ \xi_d & \widehat{C_2} & 0 & 0 & 0 & 0\\ -\sigma_{1u} & 0 & \widehat{C_3} & 0 & 0 & 0\\ 0 & -\sigma_{1d} & -\epsilon_d\ \xi_d & \widehat{C_4} & 0 & 0\\ 0 & 0 & -\sigma_{2u} & 0 & \widehat{C_5} & 0\\ 0 & 0 & 0 & -\sigma_{2d} & -\epsilon_d\ \xi_d & \widehat{C_6}\end{bmatrix}$$

where, $\hat{C_1}=\epsilon_d\ \xi_d+\sigma_{1u}+\mu, \hat{C_2}=\tau_1+\sigma_{1d}+\mu, \hat{C_3}=\epsilon_d\ \xi_d+\sigma_{2u}+\mu, \hat{C_4}=\tau_2+\sigma_{2d}+\mu, \hat{C_5}=\epsilon_d\ \xi_d+\mu$ and $\hat{C_6}=\tau_A+\ \mu$.

B.3 Proof of Theorem 3.4

Consider the model (2.1) with $\varepsilon_m c_m = 1$ and $\delta_u = \delta_d = 0$. We further assume that $\hat{\mathbb{R}}_{T_c} < 1$. The proof is also based on using a comparison theorem (Gumel et al., 2021; Lakshmikantham & Leela, 1969; Safdar et al., 2023).

The equations for the infected compartments of the special case of the model (2.1) can be re-written as:

$$\frac{d}{dt}\begin{bmatrix} I_{1_u}(t) \\ I_{1_d}(t) \\ I_{2_u}(t) \\ I_{2_d}(t) \\ A_u(t) \\ A_d(t) \end{bmatrix} = (\hat{F} - \hat{V}) \begin{bmatrix} I_{1_u}(t) \\ I_{1_d}(t) \\ I_{2_u}(t) \\ I_{2_d}(t) \\ A_u(t) \\ A_d(t) \end{bmatrix} - M \begin{bmatrix} I_{1_u}(t) \\ I_{1_d}(t) \\ I_{2_u}(t) \\ I_{2_d}(t) \\ A_u(t) \\ A_d(t) \end{bmatrix}, \tag{B.2}$$

where the next generation matrices $\hat{F}$ and $\hat{V}$ are as defined in Equation (B.2) and the matrix M is defined as:

$$M = \beta\ (S_L^* - S_L) \begin{bmatrix} 1 & \eta_d & \eta_2 & \eta_2\eta_d & \eta_A & \eta_A\eta_d \\ 0 & 0 & 0 & 0 & 0 & 0 \\ 0 & 0 & 0 & 0 & 0 & 0 \\ 0 & 0 & 0 & 0 & 0 & 0 \\ 0 & 0 & 0 & 0 & 0 & 0 \end{bmatrix}. \tag{B.3}$$

Since $S_L \leq S_L^*$ for all $t > 0$ in Γ^*, it follows that the matrix M is non-negative. Hence, Equation (B.2) can be re-written in terms of the following inequality:

$$\frac{d}{dt}\begin{bmatrix} I_{1_u}(t) \\ I_{1_d}(t) \\ I_{2_u}(t) \\ I_{2_d}(t) \\ A_u(t) \\ A_d(t) \end{bmatrix} \leq (\hat{F} - \hat{V}) \begin{bmatrix} I_{1_u}(t) \\ I_{1_d}(t) \\ I_{2_u}(t) \\ I_{2_d}(t) \\ A_u(t) \\ A_d(t) \end{bmatrix}. \tag{B.4}$$

It should be recalled from the local asymptotic stable result for the disease-free equilibrium of the model (2.1) (given in Theorem 3.1) that all eigenvalues of the associated next generation matrix FV^{-1} are negative if $\mathbb{R}_{T_c} < 1$ (i.e., $F - V$ is a stable matrix). It follows that the eigenvalues of the next generation matrix $\hat{F}\hat{V}^{-1}$, associated with this special case of the model (2.1), are also negative if $\hat{\mathbb{R}}_{T_c} < 1$ (i.e., $\hat{F} - \hat{V}$ is also a stable matrix). Thus, the linearized differential inequality system (B.4) is stable whenever $\rho(\hat{F}\hat{V}^{-1}) < 1$. Consequently (Gao et al., 2023; Gumel et al., 2006; Ngonghala et al., 2023; Safdar, 2023; Safdar et al., 2023; Sharomi et al., 2011),

$$(I_{1u}(t), I_{1d}(t), I_{2u}(t), I_{2d}(t), A_u(t), A_d(t)) \to (0, 0, 0, 0, 0, 0), \text{ as } t \to \infty.$$

Substituting $I_{1u}(t) = I_{1d}(t) = I_{2u}(t) = I_{2d}(t) = A_u(t) = A_d(t) = 0$ into the differential equations for the rate of change of the $S_L(t)$, $S_H(t)$ and $T(t)$ compartments of the model (2.1) shows that:

$$S_L(t) \to S_L^*, S_H(t) \to S_H^* \text{ and } T \to 0 \text{ as } t \to \infty.$$

Thus, the disease-free equilibrium $(\mathcal{E}_{DF})$ of the special case of the model (2.1), with $\varepsilon_p\ c_p = 1$ and $\delta_u = \delta_d = 0$ is globally-asymptotically stable in Γ^* whenever $\hat{\mathbb{R}}_{T_c} < 1$. □

References

Arizona Department of Health Services. (2015). *HIV/AIDS in Arizona integrated epidemiologic profile*. https://www.azdhs.gov/preparedness/epidemiology-disease-control/disease-integration-services/index.phphiv-epidemiology-reports. (Accessed 5 April 2023).

Arizona Department of Health Services. (2021). *HIV/AIDS in Arizona*. https://www.azdhs.gov/documents/preparedness/epidemiology-diseasecontrol/disease-integrated-services/hiv-epidemiology/reports/2021/annualreport.pdf. (Accessed 30 December 2022).

Arizona Department of Health Services. (2023). *Population health and vital statistics in Arizona*. https://pub.azdhs.gov/health-stats/menu/info/trend/index.php?pg=births. (Accessed 2 June 2023).

Biktarvy Biktarvy. (2022). https://www.biktarvy.com. (Accessed 5 April 2023).

Bingham, A., Shrestha, R. K., Khurana, N., Jacobson, E. U., & Farnham, P. G. (2021). *Estimated lifetime HIV-Related medical costs in the United States*. https://pubmed.ncbi.nlm.nih.gov/33492100/. (Accessed 15 May 2023).

Blayneh, K. W., Gumel, A. B., Lenhart, S., & Tim Clayton. (2010). Backward bifurcation and optimal control in transmission dynamics of West Nile virus. *Bulletin of Mathematical Biology, 72*, 1006–1028.

Carr, J. (2012). *Applications of centre manifold theory, ume 35*. Springer Science & Business Media.

Castillo-Chavez, C., & Song, B. (2004). Dynamical models of Tuberculosis and their applications. *Mathematical Biosciences and Engineering, 1*(2), 361–404.

Centers for Disease Control and Prevention. (2020a). *HIV testing*. https://www.cdc.gov/hiv/testing/. (Accessed 5 April 2023).

Centers for Disease Control and Prevention. (2020b). HIV transmission. https://www.cdc.gov/hiv/basics/transmission.html. (Accessed 25 February 2023).

Centers for Disease Control and Prevention. (2020c). *HIV and injection drug use*. https://www.cdc.gov/hiv/basics/hiv-transmission/injection-drug-use.html.
Centers for Disease Control and Prevention. (2021a). *Sexually transmitted infections treatment guidelines*, 2020 https://www.cdc.gov/hiv/basics/transmission.html. (Accessed 25 February 2023).
Centers for Disease Control and Prevention. (2021b). PrEP for HIV Prevention in the U.S. https://www.cdc.gov/nchhstp/newsroom/fact-sheets/hiv/PrEP-for-hiv-prevention-in-the-US-factsheet.html. (Accessed 27 March 2023)
Centers for Disease Control and Prevention. (2021c). About ending HIV epidemic in the U.S. Initiative https://www.cdc.gov/endhiv/about.html. (Accessed 5 April 2023).
Centers for Disease Control and Prevention. (2022a). *Hiv cost effectiveness*. https://www.cdc.gov/hiv/programresources/guidance/costeffectiveness/index.html. (Accessed 15 May 2023).
Centers for Disease Control and Prevention. (2022b). Prep effectiveness. https://www.cdc.gov/hiv/basics/prep/prep-effectiveness.html. (Accessed 5 April 2023).
Centers for Disease Control and Prevention. (2022c). *Deaths and mortality*. https://www.cdc.gov/nchs/fastats/deaths.htm. (Accessed 5 April 2023).
Centers for Disease Control and Prevention. (2023). Pre-exposure prophylaxis (prep) https://www.cdc.gov/hiv/risk/prep/index.html. (Accessed 27 February 2023).
Chen, L., Yang, J., Zhang, R., Xu, Y., Zheng, J., Jiang, J., Jiang, J., Lin, H., Wang, N., Yeung, P. C., et al. (2015). Rates and risk factors associated with the progression of HIV to AIDS among HIV patients from Zhejiang, China between 2008 and 2012. *AIDS Research and Therapy, 12*(1), 1–8.
Clinic, M. (2022). HIV/AIDS overview and symptoms. URL https://www.mayoclinic.org/diseases-conditions/hiv-aids/symptoms-causes/syc-20373524#:text=Untreated. (Accessed 25 February 2023).
Diekmann, O., & Peter Heesterbeek, J. A. (2000). *Mathematical epidemiology of infectious diseases: Model building, analysis and interpretation, ume 5*. John Wiley & Sons.
van den Driessche, P., & James, W. (2002). Reproduction numbers and sub-threshold endemic equilibria for compartmental models of disease transmission. *Mathematical Biosciences, 180*(1–2), 29–48.
Eisinger, R. W., Dieffenbach, C. W., & Fauci, A. S. (2019). HIV viral load and transmissibility of HIV infection: Undetectable equals untransmittable. *JAMA, 321*(5), 451–452.
Food and Drug Administration. (2019). *FDA approves second drug to prevent HIV infection as part of ongoing efforts to end the HIV epidemic*. https://www.fda.gov/news-events/press-announcements/fda-approves-second-drug-prevent-hiv-infection-part-ongoing-efforts-end-hiv-epidemic. (Accessed 5 April 2023).
Gao, S., Pant, B., Williams Chukwu, C., Kwofie, T., Safdar, S., Newman, L., Choe, S., Datta, B. K., Kwame Attipoe, W., Zhang, W., et al. (2023). A mathematical model to assess the impact of testing and isolation compliance on the transmission of covid-19. *Infectious Disease Modelling, 8*(2), 427–444.
Grey, J. A., Bernstein, K. T., Sullivan, P. S., Purcell, D. W., Chesson, H. W., Gift, T. L., & Rosenberg, E. S. (2016). Estimating the population sizes of men who have sex with men in U.S. states and counties using data from the American Community Survey. *JMIR Public Health and Surveillance, 2*(1), Article e5365.
Gumel, A. B. (2012). Causes of backward bifurcations in some epidemiological models. *Journal of Mathematical Analysis and Applications, 395*(1), 355–365.
Gumel, A. B., Iboi, E. A., Ngonghala, C. N., & Ngwa, G. A. (2021). Toward achieving a vaccine-derived herd immunity threshold for covid-19 in the U.S. *Frontiers in Public Health, 9*, Article 709369.
Gumel, A. B., McCluskey, C. C., & van den Driessche, P. (2006). Mathematical study of a staged-progression HIV model with imperfect vaccine. *Bulletin of Mathematical Biology, 68*, 2105–2128.
Hethcote, H. W. (2000). The mathematics of infectious diseases. *SIAM Review, 42*(4), 599–653.
Hood, J. E., Buskin, S. E., Julia C, D., David, A. K., Elizabeth, A. B., Katzi, D. A., & Golden, M. R. (2016). Dramatic increase in preexposure prophylaxis use among MSM in Washington state. *AIDS, 30*(3), 515–519.
J Brozak, S., Pant, B., Safdar, S., & Gumel, A. B. (2021). Dynamics of covid-19 pandemic in India and Pakistan: A metapopulation modelling approach. *Infectious Disease Modelling, 6*, 1173–1201.
Kaiser Family Foundation. (2020). *Black Americans and HIV/AIDS the basics*. https://www.KFF.org/hivaids/fact-sheet/black-americans.and.hivaids.the.basics. (Accessed 5 April 2023).
Lakshmikantham, V., & Leela, S. (1969). *Differential and integral inequalities: Theory and applications: Volume I: Ordinary differential equations*. Academic press.
M Blower, S., & Dowlatabadi, H. (1994). Sensitivity and uncertainty analysis of complex models of disease transmission: An HIV model, as an example. *International Statistical Review/Revue Internationale de Statistique*, 229–243.
Marino, S., Hogue, I. B., Ray, C. J., & E Kirschner, D. (2008). A methodology for performing global uncertainty and sensitivity analysis in systems biology. *Journal of Theoretical Biology, 254*(1), 178–196.
McCann, N. C., Horn, T. H., Hyle, E. P., & Walensky, R. P. (2020). HIV Antiretroviral therapy costs in the United States, 2012-2018. *JAMA Internal Medicine, 180*(4), 601–603.
McLeod, R. G., Brewster, J. F., Abba, B. G., & Slonowsky, D. A. (2006). Sensitivity and uncertainty analyses for a SARS model with time-varying inputs and outputs. *Mathematical Biosciences and Engineering, 3*(3), 527–544.
Mitchell, K. M., Prudden, H. J., Ramesh, B. M., Washington, R., Isac, S., Rajaram, S., Terris-Prestholt, F., & Vickerman, P. (2014). Mathematical modelling of the impact of PrEP for female sex workers and men who have sex with men upon HIV incidence and survival in Southern India. *AIDS Research and Human Retroviruses, 30*(S1), A161–A162.
National Institutes of Health. (2021). *HIV and women*. https://www.hivinfo.nih.gov/understanding-hiv/fact-sheets/hiv-and-women. (Accessed 5 April 2023).
Ngonghala, C. N., Knitter, J. R., Marinacci, L., Bonds, M. H., & Gumel, A. B. (2021). Assessing the impact of widespread respirator use in curtailing COVID-19 transmission in the USA. *Royal Society Open Science, 8*(9), Article 210699.
Ngonghala, C. N., Taboe, H. B., Safdar, S., & Gumel, A. B. (2023). Unraveling the dynamics of the Omicron and Delta variants of the 2019 coronavirus in the presence of vaccination, mask usage, and antiviral treatment. *Applied Mathematical Modelling, 114*, 447–465.
NHS. (2021). HIV/AIDS prevention. https://www.nhs.uk/conditions/hiv-and-aids/prevention/. (Accessed 25 February 2023).
Nsuami, M. U., & Peter, J. W. (2018). A model of HIV/AIDS population dynamics including ARV treatment and pre-exposure prophylaxis, 2018 *Advances in Difference Equations, 1–12*.
Omondi, E. O., Mbogo, R. W., & Luboobi, L. S. (2018). Mathematical modelling of the impact of testing, treatment and control of HIV transmission in Kenya. *Cogent Mathematics & Statistics, 5*(1), Article 1475590.
Omondi, E. O., Mbogo, R. W., & Luboobi, L. S. (2022). A mathematical model of hiv transmission between commercial sex workers and injection drug users. *Research in Mathematics, 9*(1), Article 2082044.
Our World in data. HIV/AIDS.(2019). https://ourworldindata.org/hiv-aids. (Accessed 25 February 2023).
Pitasi, M. A., Delaney, K. P., Oraka, E., Bradley, H., DiNenno, E. A., Brooks, J. T., & Joseph, P. (2018). Interval since last HIV test for men and women with recent risk for HIV infection—United States, 2006–2016. *Morbidity and Mortality Weekly Report, 67*(24), 677.
Podder, C. N., Sharomi, O., Gumel, A. B., & Strawbridge, E. (2011). Mathematical analysis of a model for assessing the impact of antiretroviral therapy, voluntary testing and condom use in curtailing the spread of HIV. *Differential Equations and Dynamical Systems, 19*(4), 283–302.
Poorolajal, J., Hooshmand, E., Mahjub, H., Esmailnasab, N., & Jenabi, E. (2016). Survival rate of AIDS disease and mortality in HIV-infected patients: A meta-analysis. *Public Health, 139*(3–12).
Safdar, S. (2023). *Mathematics of the SARS-CoV-2 pandemic. PhD thesis*. Arizona State University.
Safdar, S., & Abba, B. (2023). In , *To appear)Gumel. Book chapter in "mathematical modelling from the next generation", fields institute for research in the mathematical sciences seminar series. Jummy david and jianhong Wu*. Springer.

Safdar, S., Ngonghala, C. N., & Gumel, A. B. (2023). Mathematical assessment of the role of waning and boosting immunity against the BA. 1 Omicron variant in the United States. *Mathematical Biosciences and Engineering, 20*(1), 179–212.
Sharomi, O., Podder, C. N., Gumel, A. B., Mahmud, S. M., & Rubinstein, E. (2011). Modelling the transmission dynamics and control of the novel 2009 swine influenza (H1N1) pandemic. *Bulletin of Mathematical Biology, 73*, 515–548.
Simpson, L., & Gumel, A. B. (2017). Mathematical assessment of the role of Pre-Exposure Prophylaxis on HIV transmission dynamics. *Applied Mathematics and Computation, 293*, 168–193.
STDcenterNY. Everything you need to know about preventing HIV with PrEP. https://www.stdcenterny.com/articles/hiv-prep-mediation-practical-guide.html, 2022. (Accessed April 5, 2023).
Sun, B. K., Yoon, M., Su Ku, N., Hyung Kim, M., Song, J. E., Jin Young, A., Su Jin, J., Kim, C., Hee-Dae, K., Lee, J., et al. (2014). Mathematical modeling of HIV prevention measures including pre-exposure prophylaxis on HIV incidence in South Korea. *PLoS One, 9*(3), Article e90080.
Supervie, V., Barrett, M., Kahn, J. S., Godfrey, M., Lebogang Moeti, T., Busang, L., & Blower, S. (2011). Modeling dynamic interactions between pre-exposure prophylaxis interventions & treatment programs: Predicting hiv transmission & resistance. *Scientific Reports, 1*(1), 185.
Taylor, R. (1990). Interpretation of the correlation coefficient: A basic review. *Journal of Diagnostic Medical Sonography, 6*(1), 35–39.
Tollett, Q. (2023). *Mathematics of transmission dynamics and control of HIV/AIDS in an MSM population. PhD thesis*. Arizona State University.
UNAIDS. (2023). In *UNAIDS fact-sheet*. https://www.unaids.org/en/resources/fact-sheet. (Accessed 5 April 2023).
U.S. Department of Health & Human Services. (2021a). Pre-exposure prophylaxis. https://www.hivinfo.hiv.gov/understanding-hiv/fact-sheets/pre-exposure-prophylaxis-prep. (Accessed 25 November 2022).
U.S. Department of Health & Human Services. (2021b). *About ending the HIV epidemic: Plan for America*. https://www.hiv.gov/federal-response/ending-the-hiv-epidemic/overview. (Accessed 5 April 2023).
U.S. Department of Health & Human Services. (2022). *Pre-exposure prophylaxis*. https://www.hiv.gov/hiv-basics/hiv-prevention/using-hiv-medication-to-reduce-risk/pre-exposure-prophylaxis.
U.S. Department of Health & Human Services. (2023). *Global statistics*. https://www.hiv.gov/hiv-basics/overview/data-and-trends/global-statistics. (Accessed 8 September 2023).